# Economies of scale in ammonia synthesis loops embedded with iron- and ruthenium-based catalysts

Masaki Yoshida†, Takaya Ogawa†*, Yoko Imamura, Keiichi N. Ishihara

Graduate School of Energy Science, Kyoto University, Yoshida-honmachi, Sakyo-ku, Kyoto 606-8501, Japan

*Corresponding author: ogawa.takaya.8s@kyoto-u.ac.jp

Keywords: Ammonia synthesis process, cost analysis, economy of scales, ruthenium catalyst, renewable energy

**Abstract (150 words)**

The economies of scale were analyzed in ammonia synthesis loops embedded with iron-based catalysts (Fe) and ruthenium-based catalysts (Ru/C). Aspen Plus© was utilized to simulate the synthesis and separation processes with the product range from ammonia 0.1-500 tonne/day. The detailed kinetic models, the Temkin equation and the modified one, were employed to evaluate catalytic activity in reactors precisely. The result shows the cost advantage of Ru/C on a small scale. Besides, on a small scale, the costs of heat exchangers and reactors are dominant, while the catalyst cost of Ru/C itself is not dominant on any scales. For the ammonia synthesis based on renewable energy, Ru/C catalyst under mild pressure, i.e., Ru/C-50bar, is preferable. The direction of the future research on the catalyst of ammonia synthesis from the viewpoint of cost is also discussed.

## 1. Introduction

Ammonia is indispensable for human beings as an artificial fertilizer and is one of the most produced chemicals. The amount of ammonia production is more than 182 million tonnes in 2019 and is expected to increase by a total of 4% during the next four years [1]. Furthermore, ammonia is a carrier of renewable energy because ammonia can be synthesized from the hydrogen gas prepared by water electrolysis based on renewable energy. Ammonia is promising as a carrier because it readily becomes a liquid state under less than 10 atm at room temperature, and liquid ammonia has a high energy density in weight and volume [2-7]. Liquid ammonia is suitable for a portable fuel because nitrogen gas can be emitted into the air without pollution and obtained everywhere. It means no need to recover nitrogen gas after the utilization and send back to the location that generates hydrogen from renewable energy, which omits the cost and energy for recovery and transportation. The market size of ammonia has an enormous potential to expand in the near future.

Industrial production of ammonia is operated through the following exothermic reaction: $N_2 + 3H_2$

$\rightarrow 2NH_3$ $\Delta H = -92$ kJ/mol [8]. The production usually employs the Haber-Bosch process, where the catalyst is iron-based one, and the operation condition is harsh: 350-525 °C and 100-300 atm [9]. Although the lower temperature is favorable in terms of equilibrium, the reaction temperature must be high to accelerate the reaction. The cost of equipment, including reactors and compressors, is much expensive to endure the severe condition. These costs are usually cut down by the economy of scale [10], and thus the plant of ammonia production has been generally large and centralized, e.g., 1000 tonne/day [11].

Recently, the small-scale plants get attention, such as the plant, which produces 3, 10, and 60 tonne/day of ammonia and consumes 1.5, 5-6, and 25-30 MW, respectively [12]. The small-scale plant can reduce risks of capital investment and enables localized production. Thus, the transportation cost decreases, the safety consideration and the worse accessibility are mitigated. The local community obtains self-sufficiency and independence, avoids ammonia price fluctuations, and ensures the security of ammonia supply [12-14]. Moreover, renewable energy, which is characterized as highly distributed, is efficiently utilized in rural areas for the small-scale of ammonia synthesis [12, 14, 15]. However, the small plant sacrifices the benefits of scale, and the equipment for the harsh operating condition induces high cost. To realize the small-scale and localized plants, the moderate condition for ammonia synthesis is desired, which reduces the extreme robustness of the equipment.

The suitable catalyst for mitigating the reaction condition is ruthenium supported by graphitized carbon (Ru/C). In 1972, an alkali promoted Ru/C was invented by the Ozaki group and showed high activity at moderate conditions [16]. Plenty of researches has developed Ru/C, and its reactivity is much higher than conventional iron-based catalyst [17-25] even though the operation condition is mild: 325-450 °C and $\leq$ 100 atm [9]. Besides, recent researches significantly developed the ruthenium-based catalysts and achieved high reactivity at a surprisingly mild condition in a lab-scale [26-30]. The catalysts with various metals also show excellent activity at ambient conditions [31-37].

Ru/C has already been realized in Kellog Advanced Ammonia Process (KAAP) process, and there are enough datasets to model a reactor based on Ru/C [41, 48]. However, the plant scale of KAAP is enormous; around 2000 tonne/day [11]. In addition, the number of plants is only seven in the world, and the conventional iron-based catalysts have been still general [11]. Although many reports simulate and optimize the processes of the plants on small-scales, they employ the harsh condition needed by iron-based catalysts or assume equilibrium without consideration of real catalytic activities [13, 38-45]. The detailed kinetic model must be employed to evaluate the advantage of the Ru/C catalyst in the reaction. Furthermore, the optimization and analysis of the plants based on Ru/C are scarce, with only two literatures [46, 47]. One focuses on the optimization of the reaction [46]. The other analyzed the cost of the polygeneration process for natural gas and ammonia with the up-to-date models for Ru/C [47]. To the best of our knowledge, no research investigates the economies of scale in the plant embedded with ruthenium-based catalysts and clarify the advantage of ruthenium-based catalysts on

a small scale. The ruthenium is expensive, considered as the fatal drawback of Ru/C [9, 18]. If Ru/C mitigates reaction conditions, the cost of equipment and operation should decrease. Thus, these are a trade-off, which is influenced by the economies of scale. The quantitative investigation is required to seize the potential of ruthenium-based catalysts for small-scale plants.

In this study, we examined the economies of scale in ammonia synthesis loops embedded with Ru/C. As a comparison, the loops with the commercialized iron-based catalysts, KM1R (Fe), were also investigated. Aspen Plus© was utilized to simulate the loops and changed the amount of ammonia production scale. We implemented the detailed kinetic models as explained later to evaluate catalytic activity in reactors precisely. Several reaction conditions, including severe conditions, are assumed to compare with Fe. Based on the results, we quantitatively elucidated the advantage of Ru/C on a small scale, and identified the impact of ruthenium cost and the cost relation for electricity and equipment against scales. The direction of future research on a catalyst of ammonia synthesis from the viewpoint of cost was also suggested.

## 2. Method

### 2.1 Whole scheme of the ammonia synthesis loop

Figure 1 shows the system boundary of this study. An ammonia production plant consists of a hydrogen and nitrogen production and an ammonia synthesis loop. We focused on ammonia synthesis loop because the purpose was to evaluate the impact of the mild reaction condition achieved by Ru/C on the ammonia synthesis loop. Although the cost for hydrogen and nitrogen production process is essential, it does not change the conclusion of the comparison among all types of plants because the amount of hydrogen and nitrogen gas is the same. Therefore, in this study, the cost calculation was made for the interior of the system, the ammonia synthesis loop, while mass transfer and heat exchange took place across the boundaries of the system. (Fig1). Cryogenic air separation is suitable for preparing nitrogen gas because of high purity of nitrogen [13, 48], since the catalysts for ammonia synthesis are readily poisoned by $H_2O$ and $O_2$ [49]. Pressure swing adsorption is not suitable because it cannot achieve high purity for ammonia synthesis, although it seems preferable for small-scale production. We assumed to utilize the cold heat of $O_2$ and $N_2$ in the cryogenic air separation to cool down ammonia for the separation.

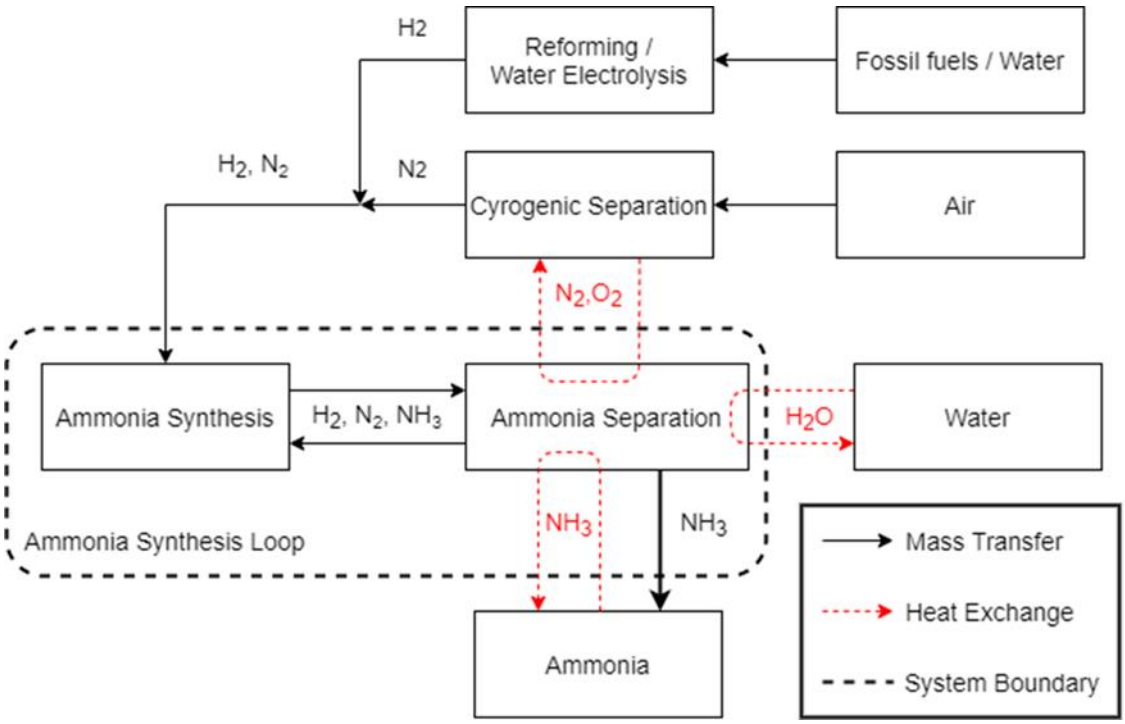


Fig. 1. The system boundary of this study, where the cost calculation was conducted for the ammonia synthesis loop.

Aspen Plus© was employed to simulate the whole processes of the ammonia synthesis loop. The loop was based on the template of the ammonia synthesis plant in Aspen Plus© with some modification (Fig. 2) [50]. The properties of gas and liquid were from the database in Aspen Plus©. The plant scales were 0.1, 1, 10, 100, and 500 tonne/day. The loops were almost the same to the plants with Fe and Ru/C to estimate how the different reaction conditions change the cost of the operation and equipment, including the catalyst cost. The inlet gas is the stoichiometric ratio of ammonia, $H_2/N_2 = 3$.

## 2.2 Multi catalyst beds and cooling system

The operation temperature in the reactor needs to be high to accelerate the reaction, although ammonia synthesis is an exothermic reaction. It means as the reaction proceeds, the temperature increases to be close to the equilibrium, and the reactivity slows down. Therefore, the reactor needs to cool down when the temperature is too high. The plant generally employs a multi-bed reactor and removes the heat in the outlet of each reactor. In this study, three beds system was applied because the three-bed reactor system was found to be the most efficient in terms of $NH_3$ production, energy savings, capital, and maintenance cost [51]. The three-bed reactor system consisted of three reactors and two heat exchangers (Fig. 2(b)).

The reactant gas before the inlet cooled the gas at the outlet of the reactor (Fig. 2(b)). The inlet and the maximum temperature (in the outlet) of each reactor were 400 °C and 490 °C for Fe and, 370 °C

and 460 °C for Ru/C, which keeps $\Delta T < 100$ K for safety [10]. These operation temperatures were determined by the available experimental data [52, 53].

In the case that the ammonia concentration is close to equilibrium, the reaction rate slowdowns and redundantly increases the reactor volume, resulting in high cost. Hence, the general way to determine the volume was employed, which stops the reaction when the product concentration reached 90% of the equilibrium under adiabatic conditions [54]. In all cases we simulated, the reactor reached to 90% of the equilibrium at the third one. The reaction was stopped when the $\Delta T$ increased to = 90 K, or the ammonia concentration in a reactor reached 90% of the equilibrium, which determines the volume of reactors.

The operation pressures were 150 and 300 bar for Fe, and 50 and 100 bar for Ru/C (hereafter Fe-150bar, Fe-300bar, Ru/C-50bar, and Ru/C-100bar, respectively), where the operation conditions are similar to the experimental data [52, 53]. The amount of produced ammonia in each scale is slightly different among the four loops, within 3%, where we considered negligible errors. The loop embedded with Ru/C under 75 bar (Ru/C-75bar) was also simulated for additional analysis.

### 2.3 Separation of ammonia by refrigeration

The ammonia concentration at equilibrium is small under high temperatures. Then, plenty of $H_2$ and $N_2$ remains unreacted and need to be recycled from the viewpoint of cost. For the recycle, we employed a general method in ammonia synthesis, refrigeration under high pressure, to make ammonia liquid and separate the product liquid and the reactant gases. The refrigeration temperature is 11.5 °C at 300 bar, –2.7 °C at 150 bar, –10.5 °C at 100 bar, and –26.0 °C at 50 bar, which was adjusted to bring the $NH_3$ molar concentration at the reactor inlet to 3 %. Water was utilized to initial cooling to room temperature (30 °C), and the cooled gases in cryogenic air separation were used in the second. To decrease temperature lower, the pressure of the $NH_3$ product was released, and its latent heat and cold heat were utilized, followed by the compression of the product to be liquid under 20 atm at room temperature, 30 °C (Fig. 2(c)). In the Fe-300 bar, the refrigeration process differs from others because the high pressure does not require much lower temperatures for ammonia separation (See Section A in the Supplementary Information).

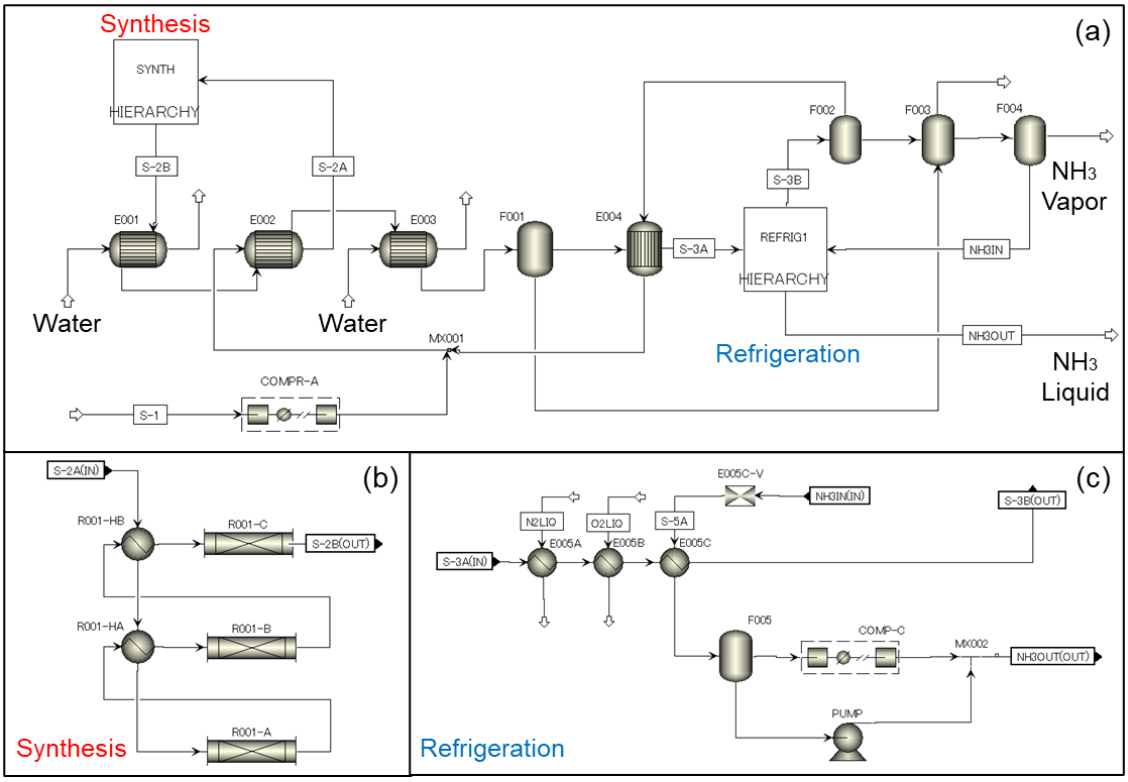


Fig. 2. (a) Overall layout of the ammonia synthesis loop simulation in Aspen Plus©. (b) Flowsheet of the ammonia synthesis process: the details of the "SYNTH" block in the overall flowsheet. (c) Flowsheet of the ammonia refrigeration process for separation of the product $NH_3$: the details of the "REFRIG1" block in the overall flowsheet.

2.4 Kinetics in a reactor

Plenty of experimental kinetic data for Fe is represented by the following simple Temkin equation [55-57]:

$$r_{NH_3} = k_r \left( K_a^2 a_{N_2} \left[ \frac{(a_{H_2})^3}{(a_{NH_3})^2} \right]^{\alpha} - \left[ \frac{(a_{NH_3})^2}{(a_{H_2})^3} \right]^{1-\alpha} \right) \quad (1)$$

where, $r_{NH_3}$ is the reaction rate in $kmol_{NH_3}/hr/m^3$of catalyst beds, $k_r$ is a kinetic constant of the reverse reaction, $K_a$ is the equilibrium constant of the reaction, $a_i$ ($i$= $H_2$, $N_2$, and $NH_3$) is the activity of component $i$, $\alpha$ is an adaptive parameter to be set at a constant value. In this study, we utilized the parameters, $\alpha$ and $k_r$, determined by Dyson et al. [55] based on the experimental kinetic data obtained by Nielsen et al. [52]. $\alpha$ is 0.5 and $k_r$ is expressed as follows:

$$k_r = 1.7698 \times 10^{15} \exp\left(-\frac{40765}{R_c T}\right) \quad (2)$$

where $R_c$ is the gas constant in cal/K/mol, the unit of the temperature $T$ is Kelvin.

The Temkin equation (1) cannot represent the experimental kinetic data for Ru-based catalysts well because the reaction over Ru-based catalysts is inhibited by hydrogen poisoning [53, 58] while the reaction over Fe-based catalysts is inhibited by ammonia poisoning [59]. Buzzi et al. considered 23 possible kinetic models by the Langmuir-Hinshelwood-Hougen-Watson (LHHW) approach, which separates the reaction into elementary reaction steps and expresses the overall reaction rate as the slowest step rate [60]. Rossetti et al. modified the Temkin equation to successfully represent the experimental kinetic data for Ru/C catalyst by the LHHW approach, which takes into account hydrogen poisoning [53]. The modified-Temkin equation under the condition of the feeding ratio $H_2/N_2 = 3$ is the following:

$$r_{N_2} = k_f \frac{\left( (a_{N_2})^{0.5} \left[ \frac{(a_{H_2})^{0.375}}{(a_{NH_3})^{0.25}} \right] - \frac{1}{K_a} \left[ \frac{(a_{NH_3})^{0.75}}{(a_{H_2})^{1.125}} \right] \right)}{1 + K_{H_2}(a_{H_2})^{0.3} + K_{NH_3}(a_{NH_3})^{0.2}} \quad (3)$$

where $r_{N_2}$ is the reaction rate in $\mathrm{kmol_{N_2}/hr/m^3}$ of catalyst beds, $k_f$ is a kinetic constant of the forward reaction, $K_{H_2}$ and $K_{NH_3}$ are the adsorption equilibrium constants for hydrogen and ammonia, respectively. The kinetic and thermodynamic parameters of Ru/C catalyst, $k_f, K_{H_2}$, and $K_{NH_3}$, have been calculated from experimental data [46, 53]:

$$k_f = 9.02 \times 10^8 \exp\left(-\frac{23000}{R_c T}\right) \quad (4)$$

$$\log_e K_{H_2} = -\frac{56.9024}{R} + \frac{37656}{RT} \quad (5)$$

$$\log_e K_{NH_3} = -\frac{34.7272}{R} + \frac{29228}{RT} \quad (6)$$

where $R$ is the gas constant in J/K/mol.

The equilibrium constant $K_a$ was calculated according to Gillespie and Beattie [53, 55, 61]:

$$\log_{10} K_a = -2.691122 \log_{10} T - 5.519265 \times 10^{-5} T + 1.848863 \times 10^{-7} T^2 + \frac{2001.6}{T} + 2.6899 \quad (7)$$

For gases, the activity of a component can be expressed as follows:

$$a_i = \frac{f_i}{P^{\ominus}} \quad (8)$$

where, $f_i$ is the fugacity of component $i$, and $P^{\ominus}$ is the standard pressure. Choosing $P^{\ominus}$ as equal to 1 atm, one can be written as:

$$a_i = f_i = \varphi_i y_i P \quad (9)$$

where $\varphi_i$ is the fugacity coefficient of component $i$, $y_i$ is the molar fraction of component $i$, $P$ is the pressure in atm. We employed the fugacity coefficients calculated by Cooper and Shaw et al. for hydrogen and by Cooper and Newton for nitrogen and ammonia [53, 55, 62, 63].

$$\varphi_{H_2} = \exp\left\{\exp(-3.8402T^{0.125} + 0.541)\,P - \exp(-0.1263T^{0.5} - 15.980)\,P^2 + 300[\exp(-0.011901T - 5.941)]\left[\exp\left(-\frac{P}{300}\right)\right]\right\} \quad (10)$$

$$\varphi_{N_2} = 0.93431737 + 0.3101804 \times 10^{-3}T + 0.295896 \times 10^{-3}P - 0.2707279 \times 10^{-6}T^2 + 0.4775207 \times 10^{-6}P^2 \quad (11)$$

$$\varphi_{NH_3} = 0.1438996 + 0.2028538 \times 10^{-2}T - 0.4487672 \times 10^{-3}P - 0.1142945 \times 10^{-5}T^2 + 0.2761216 \times 10^{-6}P^2 \quad (12)$$

The reaction kinetics, Eq. (1) for Fe-based catalysts and Eq. (3) for Ru/C catalysts, were implemented by user Fortran subroutines of the Plug flow reactor (RPlug) model in Aspen Plus©, and the "RPlug" model was adopted in adiabatic conditions.

2.5 Economic analysis

The total cost for the loops is separated into a capital cost, $C^{cap}$, and an operation cost, $C^{op}$. $C^{cap}$ was estimated by the following equations [10]:

$$C^{cap} = \sum_j C_j \quad (13)$$

$$C_j = C_{j,fix} + LM \times \frac{\text{CEPCI in 2019}}{1000} \times AF \times C_{j,ref} \times \left(\frac{s_j}{s_{ref}}\right)^{n_j} \quad (14)$$

$C_j$ is the Free On Board (FOB) cost for equipment $j$. $C_{j,fix}$ is the cost of the control system of $j$. $LM$ is the cost of labor and management. $AF$ is an alloy factor, which is determined by the cost of materials. $C_{j,ref}$ is the FOB cost for $j$ in a reference scale, $s_{ref}$. $s_j$ is the actual scale of $j$. $n_j$ is a parameter that determines the influence of a scale. The parameters in the equation (14) for each equipment, $j$, are given in Table 1 with the assumption that CEPCI is 1000. Pressure adjustment in Table 2 is multiplied to the reactor cost in a reference scale, $C_{reactor,ref}$. Stainless steel (SUS 304) was employed for the material for reactors, compressors, and heat exchangers (shell and tube) with the alloy factor, 2.75 for reactors and compressors and 2.80 for heat exchangers [10]. It is because SUS 304 is durable for the temperature and the pressure required for the plants and is tolerant for hydrogen embrittlement [64, 65]. Chemical plant cost indexes (CEPCI) in 2019, 607.5 was utilized.

Table 1. Summary of the parameter for eq. (14) [10]

| Unit | Basis | $C_{j,fix}$ | $C_{j,ref}$ | $s_{ref}$ | $n_j$ | $LM$ | $AF$ |
|---|---|---|---|---|---|---|---|
| Reactor | Volume ($m^3$) | 63,000 | 110,000 | 20 | 0.52 | 2.3 | 2.75 |
| Compressor, Low | Rated Power (kW) | 7,000 | 1,350,000 | 1000 | 0.9 | 2.15 | 2.75 |
| Compressor, High | Rated Power (kW) | 7,000 | 10,300,000 | 10000 | 0.71 | 2.15 | 2.75 |
| Heat Exchanger | Area ($m^2$) | 27,000 | 70,000 | 100 | 0.71 | 2.8 | 2.8 |

Table 2 Pressure adjustment for reactor

| P (bar) | Pressure adjustment |
|---|---|
| 300 | 6.1 |
| 150 | 3.4 |
| 100 | 2.3 |
| 75 | 1.9 |
| 50 | 1.6 |

$C^{op}$ was calculated by the following equation [10]:

$$C^{op} = \sum_{t=1}^{year} \frac{1}{(1+d)^{t-1}} C_{elec}\, E_{comp} \quad (15)$$

where the duration of the operation, *year*, is assumed as 20 years. $d$ is the discount rate, 2.25%, and $C_{elec}$ is the cost for electricity, 0.0683 USD/kWh, assuming the price for the industrial sector in 2019 in the USA [66]. The energy required to compressor per year, $E_{comp}$, is estimated by the output from Aspen Plus©.

The catalyst cost is generally estimated by weight and material cost per weight without the economy of scale [67]. In this study, the cost of the Fe and Ru/C catalysts are 0.18 USD/kg [68] and 321.04 USD/kg, respectively. The cost of Ru/C is calculated by the price of ruthenium (9730 USD/kg) and graphene (10 USD/kg) respectively [69, 70]. The Ru content was 3.2 wt% [53]. The bulk density of the Fe catalyst is 2.8 g/cm$^3$, and that of the Ru/C catalyst is 0.8 g/cm$^3$ [71]. The duration of the catalysts is assumed as ten years based on the data in the literature [17].

## 3. Results

### 3.1 Configurations of the simulated reactors

Figure 3 shows the comparison of the experimental data with the result of a single pass over the reactor simulation for validation. In the verification, a single reactor was used to investigate the ammonia conversion rates by varying the Gas Hourly Space Velocity (GHSV) at a specific temperature, pressure, and a molar ratio of hydrogen to nitrogen under experimental conditions [52, 53]. The results indicated that the conversion rates of ammonia in the simulated reactor for Fe and Ru/C were a good approximation of the ammonia conversion rates in the experiment. Therefore, the models we constructed were sufficiently accurate to describe the ammonia synthesis loops.

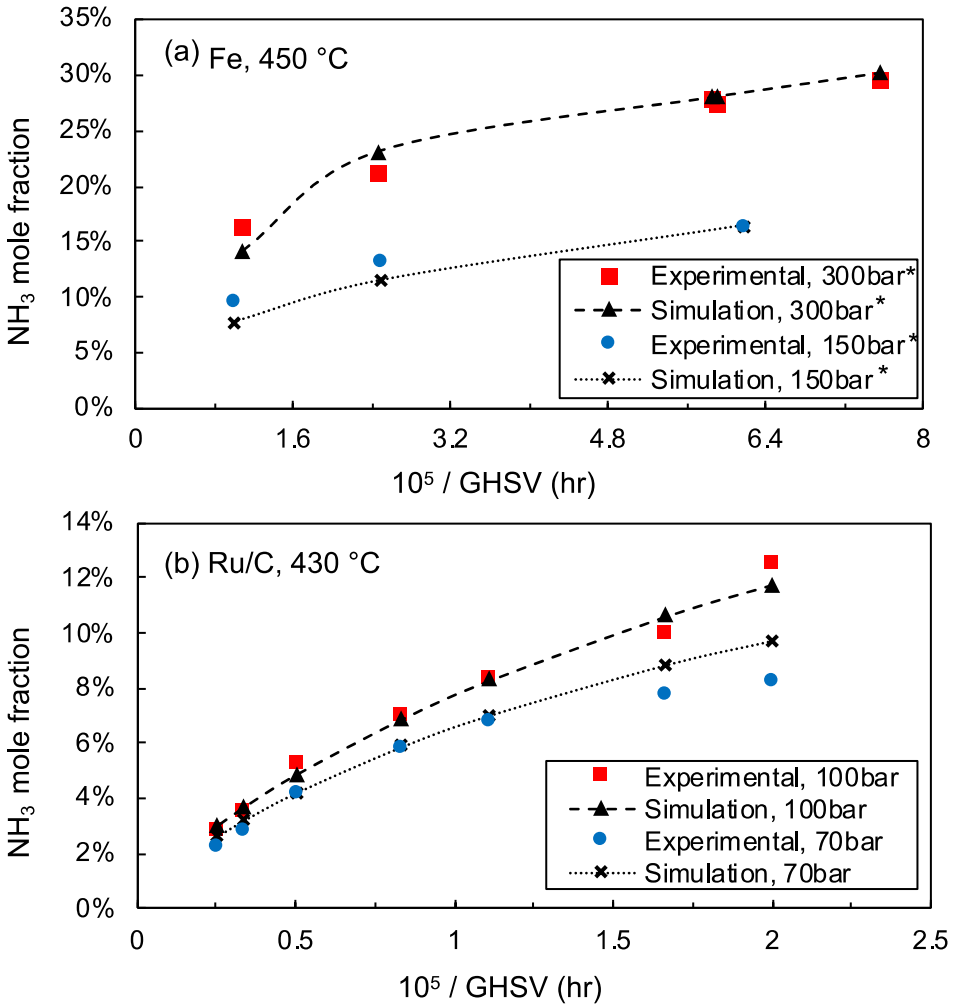


Fig. 3. Comparison of the experimental data with the reactor simulation results of a single pass over a reactor, (a) for Fe at $T$ = 450 °C, *$P$ = 304 bar (=300 atm) and 152 bar (=150 atm), and $H_2/N_2$ = 3.0 [52], (b) for Ru/C $T$ = 430 °C, $P$ = 100 bar and 70 bar, and $H_2/N_2$ = 3.0 [53].

Figure 4 shows the ammonia concentration and temperature change in the three-bed reactor in the ammonia synthesis loops. The ammonia concentration at the three-bed reactor outlet is highest at Fe-300 bar, lowest at Ru/C-50bar, and close to that at Fe-150bar and Ru/C-50bar. The total reactor size in Ru/C-100bar is smaller than that in Fe-150bar because the activity of the Ru/C catalyst at 100 bar is greater than that of the Fe-based catalyst at 150 bar (Table 3).

The tendencies in these reactors are explained by the characteristics of these catalysts and ammonia as follows. As the reactor pressure decreases, the ratio of the first bed volume to the total reactor volume tends to decrease. For Fe-300bar and Fe-150bar, the proportion of the second and third beds is large due to the reaction rate reduced by ammonia poisoning, which is severe at high pressure [59]. Then, it increases residence time and expands the volume of the second and third beds. In contrast,

Ru/C we employed tends to suffer from hydrogen poisoning rather than ammonia poisoning [58], which induces a slow reaction rate in the first reactor enriched by hydrogen but fast in the third one with a high concentration of ammonia. Hence, Ru/C results in a large volume in the first reactor and a small volume in the third one. In the comparison between Ru/C-100bar and Ru/C-50bar, the low pressure in Ru/C-50bar seems unfavorable for equilibrium to obtain a high concentration of ammonia because the reaction of Ru/C-50bar is stopped by the reason that ammonia concentration reaches 90% of equilibrium rather than $\Delta T = 90K$ even at the first and second stage. Especially, $\Delta T$ in the second reactor is small, which stops its reaction early and results in a small volume against the total. Therefore, the tendencies in these reactors are reasonable, and thus our models can well describe the properties of these catalysts.

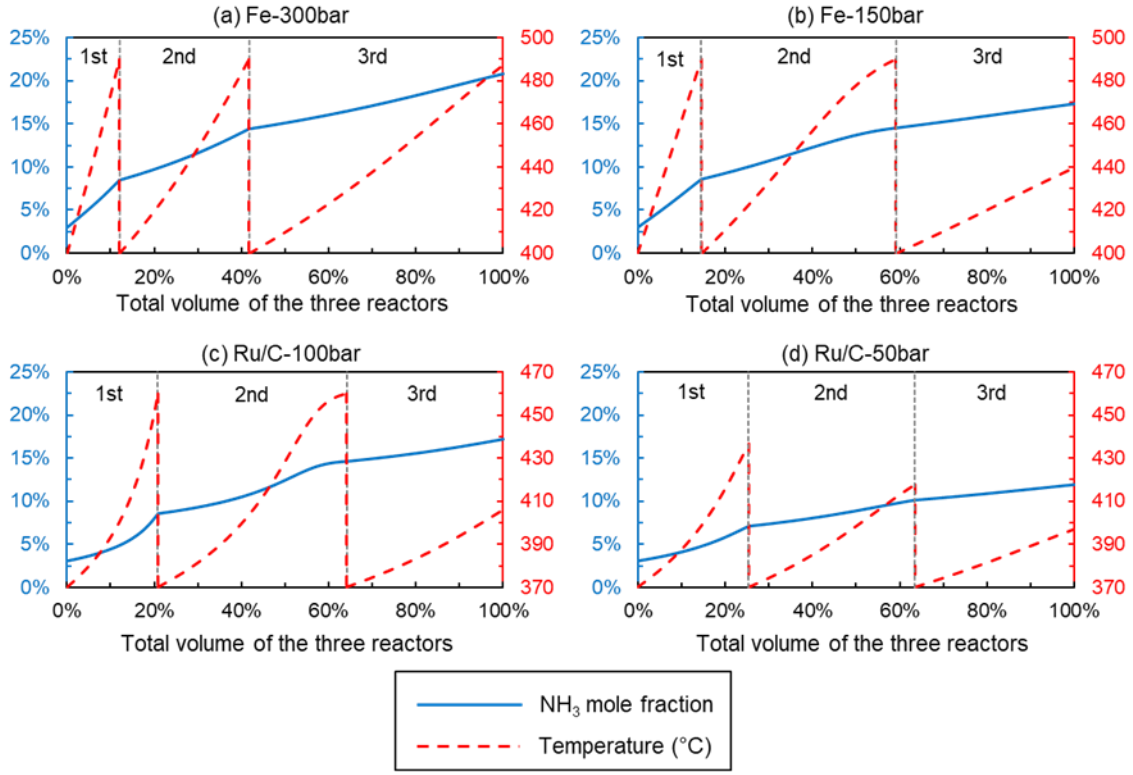


Fig. 4. $NH_3$ concentration and temperature change in the simulated three-bed reactor system in the ammonia synthesis loops, (a) Fe-300bar, (b) Fe-150bar, (c) Ru/C-100bar, (d) Ru/C-50bar.

279 Table 3. The results in the reactor system in different plant types at the scale of 100 tonne/day.

| Plant type | Temperature (°C) | Total volume of the reactors ($m^3$) | Catalyst weight (tonne) | GHSV*[1] ($10^4$ /hr) | Effluent $NH_3$ (vol.%) | Productivity*[2] (mmol/hr/$g_{cat}$) |
|---|---|---|---|---|---|---|
| Fe-300bar | 400-490 | 1.15 | 3.23 | 3.28 | 20.79 | 76.94 |
| Fe-150bar | 400-490 | 4.22 | 11.81 | 1.09 | 17.36 | 21.23 |
| Ru/C-100bar | 370-460 | 3.95 | 3.16 | 1.18 | 17.17 | 79.42 |
| Ru/C-50bar | 370-437 | 7.05 | 5.64 | 1.18 | 11.96 | 44.64 |

280 *[1] GHSV was calculated based on the total volume of the reactors ($m^3$) and the volume flow rate
281 ($m^3$/hr) of the gas flowing into the reactor system under the standard condition of 0 °C and 1 atm.
282 *[2] Productivity was calculated based on the catalyst weight ($g_{cat}$) and the molar increase in $NH_3$
283 (mmol/hr) in the gas between the reaction system inlet and outlet.
284
285 3.2 Overall cost of ammonia synthesis loop
286 Figure 5 shows the overall cost of the ammonia synthesis loops embedded with Fe and Ru/C with
287 various scales of ammonia production. Figure 6 exhibits the ratio of the total cost per the cost of Ru/C-
288 100bar. The total costs are mostly linear with the scale. Fe-300bar has the highest cost over the scale
289 of 1 tonne/day. It is noted that Fe-150bar shows the lowest cost in the scale at 500 tonne/day, and
290 Ru/C-50bar has the lowest cost at 100 tonne/day, and Ru/C-100bar shows the lowest cost below the
291 10 tonne/day scale. Therefore, it is correct that Ru/C is more advantageous than Fe in the small scale
292 of ammonia production, particularly below 100 tonne/day. However, the difference is not so large with
293 the current condition.

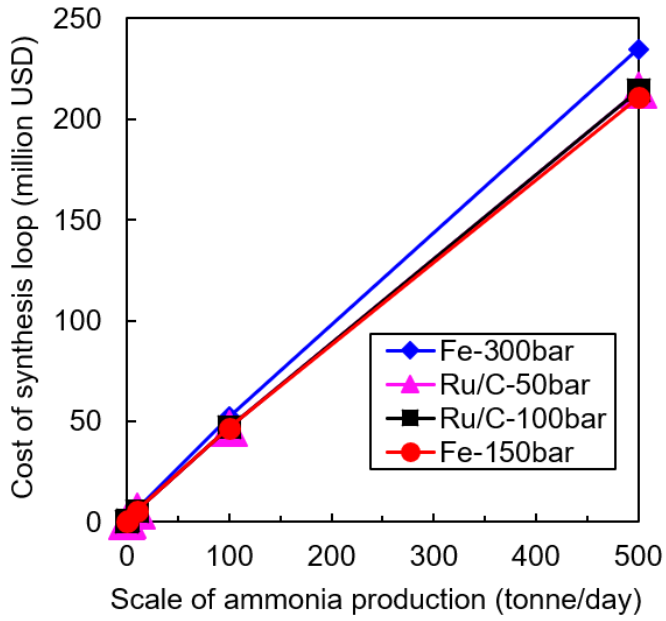


294
295 Fig. 5 The total cost of the ammonia synthesis loop against the production scale.

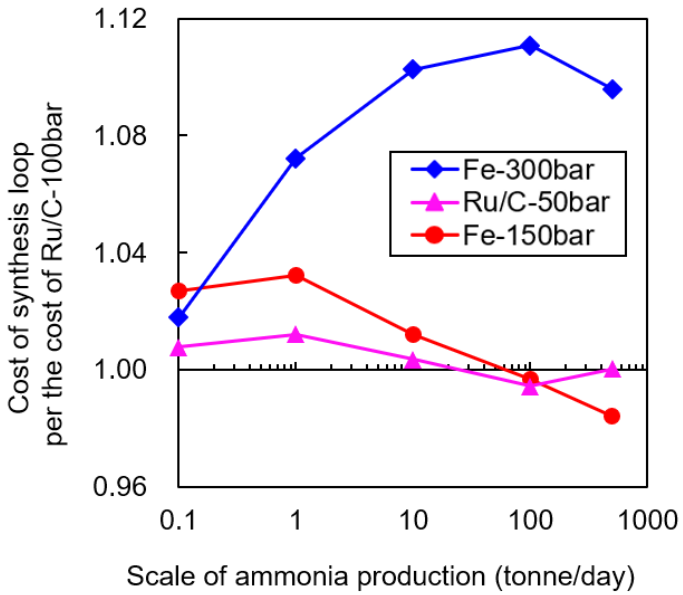


Fig. 6 The total cost of the ammonia synthesis loop per the cost of Ru/C-100bar against the production scale.

### 3.3 Breakdown of loop cost at different scales

The breakdowns of the cost of these ammonia synthesis loops are shown in Fig. 7. As general tendencies, the costs of energy consumption dominate on large scales, explaining the linear relation between the total costs and the scale because energy consumption shows mostly monotonic increases of cost. In contrast, the costs of reactors and heat exchangers are dominant on small scales. The origin that Ru/C-100bar is lower cost than Fe-150bar in the 0.1-10 tonne/day scale is all components except for catalysts are cheaper in the Ru/C-100bar than those in the Fe-150bar, and the cost of catalysts are not dominant.

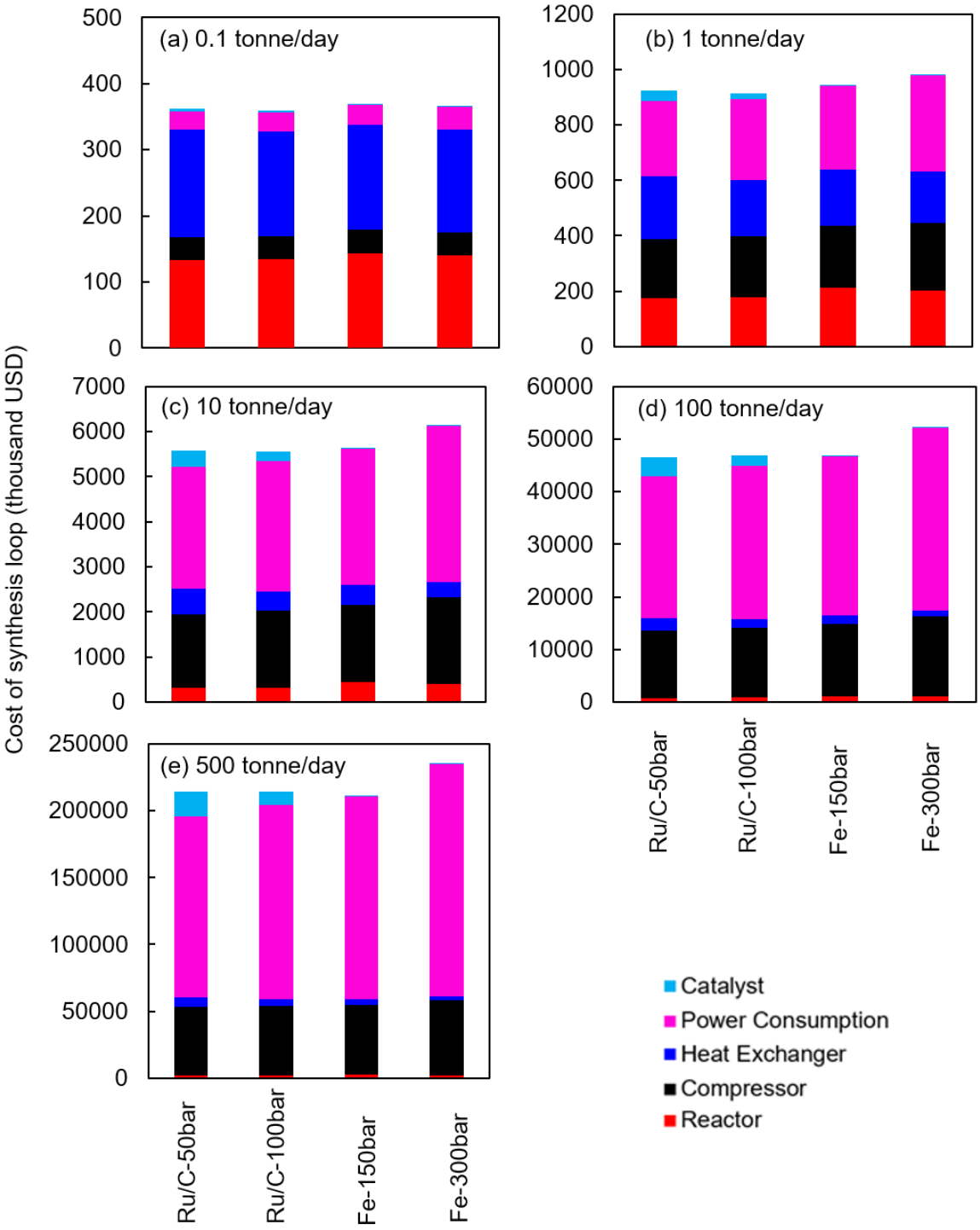


Fig. 7 Breakdown of the cost of ammonia synthesis loop in different scales, (a) 0.1 tonne/day, (b) 1 tonne/day, (c) 10 tonne/day, (d) 100 tonne/day, (e) 500 tonne/day.

The difference between Ru/C and Fe is that Fe requires large energy consumption for the harsh condition, and Ru/C induces high costs for the catalyst itself. However, the cost ratio of catalysts in Ru/C is 9 % at most, and thus the catalyst cost does not matter. Although the catalyst cost of Ru is said too expensive to be fatal, our results show that other components are higher cost. Currently, we assumed that the durability of catalysts is ten years. The other publications indicate that the catalysts can last longer than ten years [17], and then the cost ratio of catalysts will be less than 9 %. Therefore, it is concluded that the utilization of Ru metals as Ru/C is not problematic in terms of cost.

### 3.4 Sensitivity to the electricity price, catalyst cost, and pressure

This section analyzes the sensitivities of parameters in each case, and preferable cases are suggested in the different conditions. The energy consumption is dominant, more than 30%, except for a tiny scale, 0.1 tonne/day. Then, we analyzed the change of sensitivity against energy price. The current price of electricity is assumed to be the industrial price in the USA, which is variable based on locations. Figure 8 exhibited the change in total cost when the energy price increased to 110%. The least sensitive one to energy price is the loop with Ru/C-50bar. It means that Ru/C is advantageous in the case that the price of electricity is high. When the energy price increased to 106.3%, i.e., 0.0726 USD/kWh, the cost of Ru/C-50bar is the same as the cost of Ru/C-100bar at the scale of 10 tonne/day. Hence, if the price is more than 0.0726 USD/kWh, Ru/C-50bar is the cheapest at a 10 tonne/day scale.

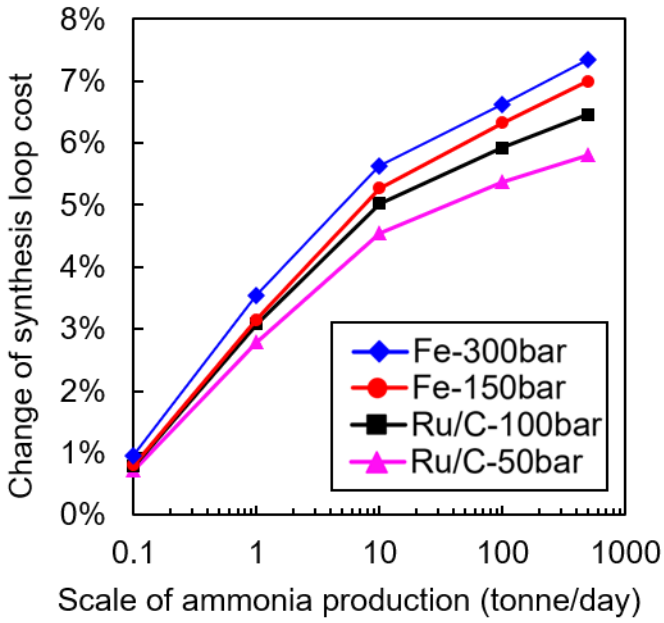


Fig. 8. The sensitivities of synthesis loop cost when energy price increases by 10% (i.e., the case that the energy price increased from 0.0683 USD/kWh to 0.07513 USD/kWh).

The catalyst cost for Ru/C-50bar is relatively high. Figure 9 indicates the sensitivities on the cost where the catalyst cost is twice, or the loading amount of the catalyst is double, or the lifetime of the catalyst becomes half. In this case, with Ru/C-50bar, the catalyst cost at a 500 tonne/day scale is 17% in the total and cannot be ignored.

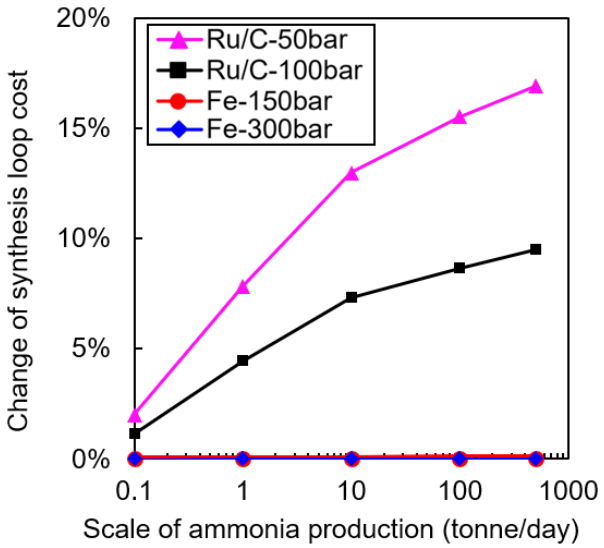


Fig. 9. The sensitivities of synthesis loop cost due to the twice cost for catalyst

Figure 10 shows the cost of each component against pressure at the loop embedded with Ru/C. The costs of power consumption and compressor are high at high pressure. The catalyst cost is small at high pressure because the reaction rate is fast at the condition, and fewer catalysts are required. It is noted that the cost of heat exchangers increases when the pressure is mild. It is derived from that the unreacted gas increases due to slow reaction rate at small pressure, and needs to be more recycled, and thus the total volume in the loop also increases (Table 4). In contrast, the difference in the cost of the reactors among three pressure is within 1% even though the volume of a reactor also increases due to low pressure. It is because of the pressure adjustment, which is applied for the only reactor.

As a summary of this section, in the case that electricity price is high, the mild pressure achieved by Ru/C is preferable to reduce energy consumption. Still, it requires more catalysts and a large volume of a heat exchanger, resulting in a high cost. These are in the trade-off relation.

352 Table 4. Scales of reactors and heat exchangers in the loop embedded with Ru/C (Please see Table
353 A.2. in Supplementary Information for details)

| | | 10 tonne/day | | | 100 tonne/day | | |
|---|---|---|---|---|---|---|---|
| | Unit | 100 bar | 75 bar | 50 bar | 100 bar | 75 bar | 50 bar |
| Reactor | Total volume ($m^3$) | 0.395 | 0.477 | 0.705 | 3.954 | 4.770 | 7.050 |
| Heat exchanger | Total area ($m^2$) | 38.9 | 53.2 | 68.4 | 388.6 | 531.6 | 684.4 |
| Molar flow rate* | $10^5$ mol/hr | 2.08 | 2.50 | 3.15 | 20.80 | 24.97 | 31.51 |

354 * The molar flow rate of gas into the reactor system

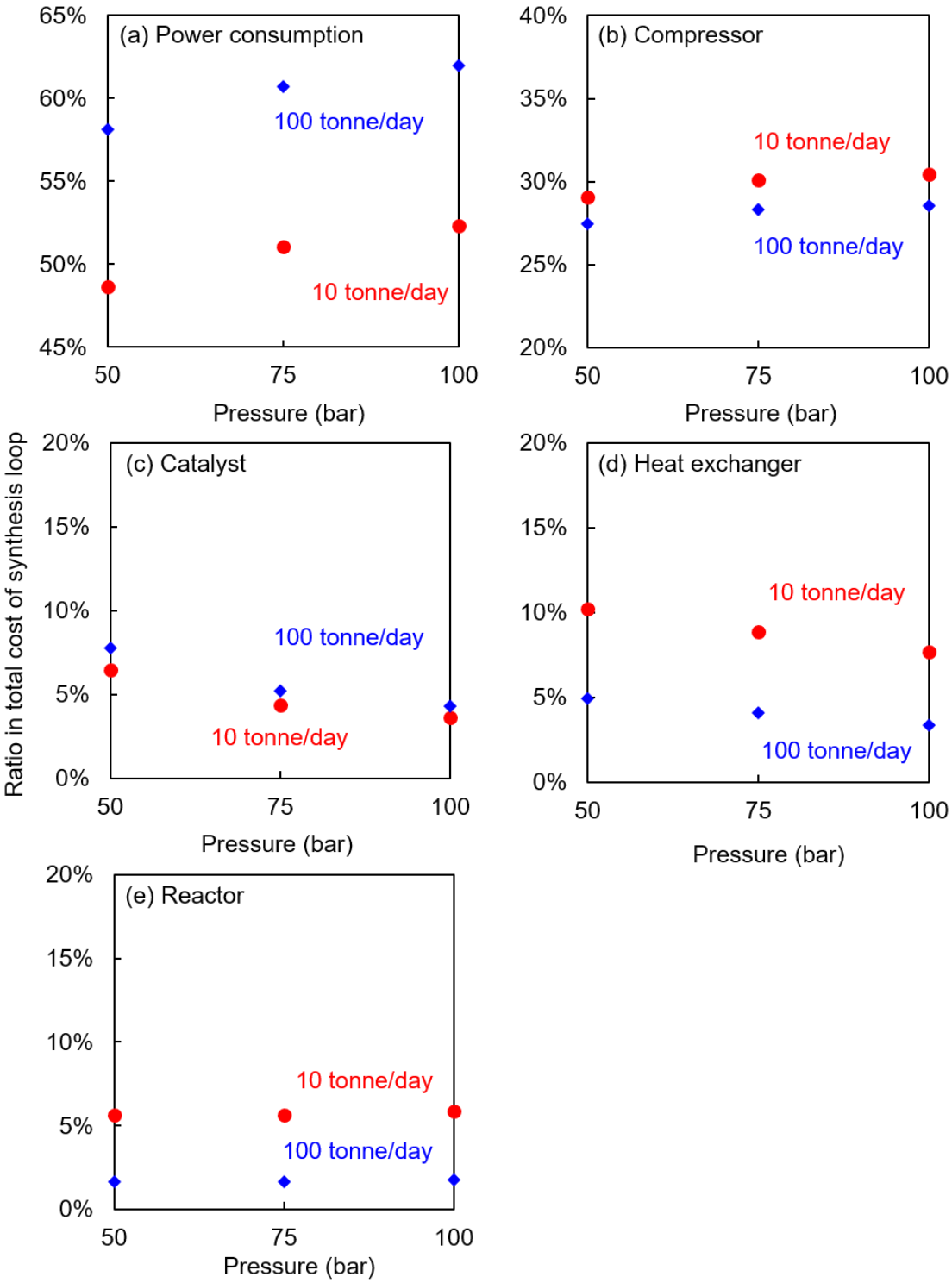


Fig. 10. The ratio of each component in the total cost of the synthesis loop against operating pressure, (a) Power consumption, (b) Compressor, (c) Catalyst, (d) Heat exchanger, (e) Reactor.

### 3.5 Disadvantage of low pressure for ammonia separation

Ru/C successfully makes the reaction condition mild and decreases the cost of components. It reduces the cost of power consumption to compress inlet gas. However, the cost reduction was not drastically because low pressure is not favorable for the separation step. High pressure or low temperature are required to make ammonia liquid state, which results in large power consumption. Figure 11 indicates the total cost for ammonia separation, including heat exchanger, compressor, and power for a compressor in the separation step (See Section B in the Supplementary Information). The low pressure at milder conditions suffers from the high cost for the separation, especially in lower scales. Therefore, the cost reduction based on a milder condition in reactors is the trade-off relation with separation cost. It is derived from the property of ammonia and is inevitable without another approach, such as adsorbent. The adsorbent can separate ammonia regardless of operation pressure and release ammonia by waste heat from the loop, which is promising to reduce the power consumption for the separation.

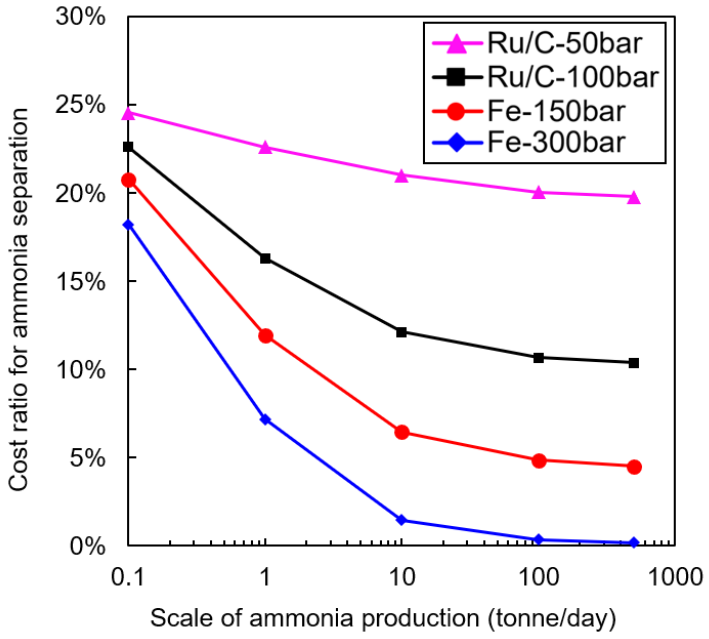


Fig. 11. Cost ratio for ammonia separation

## 4. Discussion

### 4.1 Suitable catalyst and condition for ammonia synthesis at various scales and locations

The analysis of loop cost and the cost structure against different scales reveals that the suitable catalyst and operation condition differs on the required scale and the energy prices. With the current assumption, Fe-150bar has the lowest cost in the range of over 100 tonne/day while Ru/C-50bar exhibits the lowest cost at 100 tonne/day, and Ru/C-100bar shows the lowest cost below the scale of 10 tonne/day. According to chapter 9 in the literature [17], small- and medium-scale plants employ higher operation pressure than large-scale plants. Although the reason was not clearly shown in the literature, the tendency is the same with our results where Ru/C-100bar is cheaper than Ru/C-50bar at the scale below 10 tonne/day due to the separation process. It suggests the industrial design requires high pressure at a small scale due to the ammonia separation and support the validity of our results.

It is noted that the cost structure is different from each other. As indicated in section 3.4, Ru/C-50bar is less sensitive to the cost of energy consumption. In the location that the price of electricity is high, Ru/C-50bar will be preferable, whereas the mild pressure induces high catalyst costs. Renewable energy tends to be expensive than the electricity generated by fossil fuels and is distributed with low energy density, which results in small scales. In small scales, the catalyst cost of Ru/C is not dominant, as mentioned in section 3.3. Therefore, we can conclude that the loop embedded with high loading Ru/C catalyst at mild pressure is the best for small-scale production based on renewable energy.

Recently, the cost of renewable energy is decreasing significantly. The project-level levelized cost of electricity generated by solar photovoltaics is 0.0680 USD/kWh in 2019, calculated with "*a real weighted average cost of capital; 7.5% for Organization for Economic Co-operation and Development (OECD) countries and China and 10% for the rest of the world*" [72]. It is very close to the price employed in the model is 0.0683 USD/kWh. The low cost is usually derived from the large-scale installation, which is different from the small-scale production mentioned above. Ru/C catalyst will be practical for the ammonia synthesis by the distributed generation of electricity based on renewable energy.

### 4.2 Direction for future research of ammonia synthesis

#### *4.2.1 Mild condition for ammonia synthesis achieved by recent ruthenium-based catalysts*

Here we discuss the cost reduced by the other promising catalysts. Recent progress on the ruthenium-based catalysts enables ammonia synthesis at remarkably mild conditions, such as 50 °C at 1 atm (≈ 1bar) [26]. In that condition, hydrogen embrittlement will not occur, which is fatal in the harsh condition. We currently employ SUS 304, which is durable in severe conditions and tolerant for hydrogen embrittlement. The alloy factor of SUS 304 is around 2.8, which means if the mild condition is achieved, the alloy factor decrease to 1.0 [10]. Otherwise, the materials with high thermal conductivity, such as aluminum or copper, can be utilized for heat exchangers. These can reduce the

cost of equipment. Under a small scale such as 1 tonne/day, the cost of component is more dominant than that of energy consumption. Therefore, the reduced alloy factor or the material with high thermal conductivity will be a significant impact on the total cost on a small scale. In addition, low pressure does not require the high energy to compress a gas, and then is suitable for the ammonia synthesis based on expensive energy, i.e., renewable energy.

However, low pressure induces the difficulty of ammonia separation, as shown in section 3.5. Although these are in the trade-off relation, moderate pressure, such as 10 bar, would be preferable rather than 1 bar.

As for ammonia separation, absorbent could be helpful, which can catch ammonia even under low pressure and release it by waste heat of the loop [73, 74]. Absorbent has an impact on mitigating the demerit of reduced pressure.

*4.2.2 Alternative metals for ruthenium*

Recent researches also focus on alternative catalyst metal instead of ruthenium [31, 32, 75-77]. If the ruthenium-based catalysts are durable over ten years, the cost of ruthenium is not dominant, as shown in section 3.3. However, if they deactivate within ten years or the loading amount is much more than 3.2 wt%, the catalyst impacts the total cost. Then, research to achieve a long lifetime of catalysts and reduce the loading amount of ruthenium should be focused on as well as the search for alternative metals. The cost reduction based on decreasing the amount of ruthenium and using alternative metal is the trade-off with the reactivity of the catalyst.

In the case that the energy price is high such as the usage of renewable energy, milder pressure is preferred, but more amount of catalysts is required. Thus, the recent study on making synthesis condition mild is suitable for the synthesis based on renewable energy.

*4.2.3 Catalyst without ammonia poisoning*

As shown in Fig. 4, ammonia concentration is finally high in the third reactors. Fe has a negative reaction order for ammonia [59], which means Fe is poisoned by ammonia and is not suitable for the synthesis at a high ammonia concentration. Remarkable catalysts in the recent researches have a negative order [29, 31, 32], as well as Fe. In contrast, Ru/C has almost zero reaction order for ammonia and is ideal for the third reactor [58]. The catalysts without ammonia poisoning should be invented for efficient synthesis. With this point of view, the catalyst, Ru/Ba/LaCeO, has almost zero-order and is promising [78].

## 5. Conclusion

This study performed the economic analysis of the ammonia synthesis loops embedded with Fe and Ru/C at a broad production scale under several operating conditions. It elucidated that Fe-150bar is

the lowest cost on a large scale, 500 tonne/day range. Ru/C-50bar is the lowest at 100 tonne/day scale, and Ru/C-100bar exhibits the lowest cost under a 100 tonne/day scale. These suggest that Ru/C is advantageous on the small scales, especially below 100 tonne/day scale. Furthermore, in contrast to the general idea that ruthenium is too expensive, the catalyst cost of ruthenium is not dominant on any scale. If the recent ruthenium-based catalyst has a short lifetime, or the loading amount of ruthenium is much more than 3.2%, the research of alternative metal to reduce the catalyst cost of ruthenium is practical. The research on the new catalyst to mitigate the operation condition is promising to reduce the cost of reactor and heat exchanger, but too small pressure also induces the high cost. Moderate pressure, such as 10 bar, will be preferable, which is also advantageous to separate ammonia. For the ammonia synthesis based on renewable energy, which is distributed and expensive, Ru/C catalyst under mild pressure, i.e., Ru/C-50bar, is preferable. The other promising catalysts in the recent researches are also beneficial to mitigate the condition and reduce the cost, which will be the focus of the next research. This study clarified the clear and quantitative advantage of Ru/C catalysts at small scales. It provides the direction for future research on the economic-effective catalyst for ammonia synthesis.

**Author Contributions**

[†]M. Y. and T. O. contributed equally to this work

**Acknowledgment**

This research was supported by the Environment Research and Technology Development Fund (JPMEERF20192R02) of the Environmental Restoration and Conservation Agency of Japan.

**References**

[1] U.S. Geological Survey,. Mineral commodity summaries 2020. 2020. p. 116-7.

[2] Zhao Y, Setzler BP, Wang J, Nash J, Wang T, Xu B, et al. An efficient direct ammonia fuel cell for affordable carbon-neutral transportation. Joule. 2019. https://doi.org/10.1016/j.joule.2019.07.005

[3] Lamb KE, Dolan MD, Kennedy DF. Ammonia for hydrogen storage; A review of catalytic ammonia decomposition and hydrogen separation and purification. Int. J. Hydrog. Energy. 2019;44:3580-93. https://doi.org/10.1016/j.ijhydene.2018.12.024

[4] Kojima Y. Hydrogen storage materials for hydrogen and energy carriers. Int. J. Hydrog. Energy. 2019;44:18179-92. https://doi.org/10.1016/j.ijhydene.2019.05.119

[5] Lan R, Irvine JTS, Tao S. Ammonia and related chemicals as potential indirect hydrogen storage materials. Int. J. Hydrog. Energy. 2012;37:1482-94.

[6] Kobayashi H, Hayakawa A, Somarathne KD Kunkuma A, Okafor Ekenechukwu C. Science and technology of ammonia combustion. Proc. Combust. Inst. 2019;37:109-33.

https://doi.org/10.1016/j.proci.2018.09.029
[7] Wijayanta AT, Oda T, Purnomo CW, Kashiwagi T, Aziz M. Liquid hydrogen, methylcyclohexane, and ammonia as potential hydrogen storage: Comparison review. Int. J. Hydrog. Energy. 2019;44:15026-44. https://doi.org/10.1016/j.ijhydene.2019.04.112
[8] Atkins PW, De Paula J, Keeler J. Atkins' physical chemistry. 11th ed: Oxford University Press; 2018.
[9] Liu HZ. Ammonia synthesis catalyst 100 years: Practice, enlightenment and challenge. Chin. J. Catal. 2014;35:1619-40. https://doi.org/10.1016/S1872-2067(14)60118-2
[10] Woods DR. Rules of thumb in engineering practice. Wiley-VCH Verlag GmbH & Co KGaA; 2007.
[11] Brown DE, Edmonds T, Joyner RW, McCarroll JJ, Tennison SR. The genesis and development of the commercial BP doubly promoted catalyst for ammonia synthesis. Catal. Lett. 2014;144:545-52. https://doi.org/10.1007/s10562-014-1226-4
[12] Proton Ventures, Sustainable ammonia for food and power. Nitrogen+Syngas. 2018;354:1.
[13] Frattini D, Cinti G, Bidini G, Desideri U, Cioffi R, Jannelli E. A system approach in energy evaluation of different renewable energies sources integration in ammonia production plants. Renewable Energy. 2016;99:472-82. https://doi.org/10.1016/j.renene.2016.07.040
[14] Pepermans G, Driesen J, Haeseldonckx D, Belmans R, D'haeseleer W. Distributed generation: definition, benefits and issues. Energy Policy. 2005;33:787-98. https://doi.org/10.1016/j.enpol.2003.10.004
[15] U.S. Environmental Protection Agency. Distributed generation of electricity and its environmental impacts, https://www.epa.gov/energy/distributed-generation-electricity-and-its-environmental-impacts; 2017 [accessed 31 August 2020].
[16] Aika K, Ozaki A, Hori H. Activation of nitrogen by alkali-metal promoted transition-metal I. Ammonia synthesis over ruthenium promoted by alkali-metal. J. Catal. 1972;27:424-31. https://doi.org/10.1016/0021-9517(72)90179-0
[17] Liu H. Ammonia synthesis catalysts: Innovation and practice: Chemical Industry Press World Scientific; 2013.
[18] Saadatjou N, Jafari A, Sahebdelfar S. Ruthenium nanocatalysts for ammonia synthesis: A review. Chem. Eng. Commun. 2015;202:420-48. https://doi.org/10.1080/00986445.2014.923995
[19] Aika K-i. Role of alkali promoter in ammonia synthesis over ruthenium catalysts—Effect on reaction mechanism. Catal. Today. 2017;286:14-20. https://doi.org/10.1016/j.cattod.2016.08.012
[20] Rarog W, Kowalczyk Z, Sentek J, Skladanowski D, Zielinski J. Effect of K, Cs and Ba on the kinetics of $NH_3$ synthesis over carbon-based ruthenium catalysts. Catal. Lett. 2000;68:163-8. https://doi.org/10.1023/A:1019024629261
[21] Liang CH, Wei ZB, Xin Q, Li C. Ammonia synthesis over Ru/C catalysts with different carbon supports promoted by barium and potassium compounds. Appl. Catal., A. 2001;208:193-201. https://doi.org/10.1016/S0926-860X(00)00713-4
[22] Rarog-Pilecka W, Miskiewicz E, Szmigiel D, Kowalczyk Z. Structure sensitivity of ammonia synthesis

519 over promoted ruthenium catalysts supported on graphitised carbon. J. Catal. 2005;231:11-9.
520 https://doi.org/10.1016/j.jcat.2004.12.005
521 [23] Song Z, Cai TH, Hanson JC, Rodriguez JA, Hrbek J. Structure and reactivity of Ru nanoparticles
522 supported on modified graphite surfaces: A study of the model catalysts for ammonia synthesis. J. Am.
523 Chem. Soc. 2004;126:8576-84. https://doi.org/10.1021/ja031718s
524 [24] Rarog-Pilecka W, Szmigiel D, Kowalczyk Z, Jodzis S, Zielinski J. Ammonia decomposition over the
525 carbon-based ruthenium catalyst promoted with barium or cesium. J. Catal. 2003;218:465-9.
526 https://doi.org/10.1016/S0021-9517(03)00058-7
527 [25] Xu Q-C, Lin J-D, Li J, Fu X-Z, Yang Z-W, Guo W-M, et al. Combination and interaction of ammonia
528 synthesis ruthenium catalysts. J. Mol. Catal. A: Chem. 2006;259:218-22.
529 https://doi.org/10.1016/j.molcata.2006.06.030
530 [26] Hattori M, Iijima S, Nakao T, Hosono H, Hara M. Solid solution for catalytic ammonia synthesis from
531 nitrogen and hydrogen gases at 50 degrees C. Nat. Commun. 2020;11:2001.
532 https://doi.org/10.1038/s41467-020-15868-8
533 [27] Ogawa T, Kobayashi Y, Mizoguchi H, Kitano M, Abe H, Tada T, et al. High electron density on Ru in
534 intermetallic $YRu_2$: The application to catalyst for ammonia synthesis. J. Phys. Chem. C. 2018;122:10468-
535 75. https://doi.org/10.1021/acs.jpcc.8b02128
536 [28] Hara M, Kitano M, Hosono H. Ru-Loaded C12A7:$e^-$ Electride as a catalyst for ammonia synthesis.
537 ACS Catal. 2017;7:2313-24. https://doi.org/10.1021/acscatal.6b03357
538 [29] Kitano M, Inoue Y, Yamazaki Y, Hayashi F, Kanbara S, Matsuishi S, et al. Ammonia synthesis using a
539 stable electride as an electron donor and reversible hydrogen store. Nat. Chem. 2012;4:934-40.
540 https://doi.org/10.1038/nchem.1476
541 [30] Shimoda N, Kimura Y, Kobayashi Y, Kubota J, Satokawa S. Ammonia synthesis over yttrium-doped
542 barium zirconate and cerate-based perovskite-type oxide supported ruthenium catalysts. Int. J. Hydrog.
543 Energy. 2017;42:29745-55. https://doi.org/10.1016/j.ijhydene.2017.10.108
544 [31] Ye T-N, Park S-W, Lu Y, Li J, Sasase M, Kitano M, et al. Vacancy-enabled $N_2$ activation for ammonia
545 synthesis on an Ni-loaded catalyst. Nature. 2020;583:391-5. https://doi.org/10.1038/s41586-020-2464-9
546 [32] Wang P, Chang F, Gao W, Guo J, Wu G, He T, et al. Breaking scaling relations to achieve low-
547 temperature ammonia synthesis through LiH-mediated nitrogen transfer and hydrogenation. Nat. Chem.
548 2017;9:64-70. https://doi.org/10.1038/nchem.2595
549 [33] Ashida Y, Arashiba K, Nakajima K, Nishibayashi Y. Molybdenum-catalysed ammonia production with
550 samarium diiodide and alcohols or water. Nature. 2019;568:536-40. https://doi.org/10.1038/s41586-019-
551 1134-2
552 [34] Yandulov DV, Schrock RR. Catalytic reduction of dinitrogen to ammonia at a single molybdenum
553 center. Science. 2003;301:76-8. https://doi.org/10.1126/science.1085326
554 [35] Wickramasinghe LA, Ogawa T, Schrock RR, Müller P. Reduction of dinitrogen to ammonia catalyzed

555 by molybdenum diamido complexes. J. Am. Chem. Soc. 2017;139:9132-5.
556 https://doi.org/10.1021/jacs.7b04800
557 [36] Anderson JS, Rittle J, Peters JC. Catalytic conversion of nitrogen to ammonia by an iron model
558 complex. Nature. 2013;501:84-7. https://doi.org/10.1038/nature12435
559 [37] Arashiba K, Miyake Y, Nishibayashi Y. A molybdenum complex bearing PNP-type pincer ligands leads
560 to the catalytic reduction of dinitrogen into ammonia. Nat. Chem. 2011;3:120-5.
561 https://doi.org/10.1038/nchem.906
562 [38] Sánchez A, Martín M. Scale up and scale down issues of renewable ammonia plants: Towards modular
563 design. Sustainable Prod. Consumption. 2018;16:176-92. https://doi.org/10.1016/j.spc.2018.08.001
564 [39] Al-Zareer M, Dincer I, Rosen MA. Transient analysis and evaluation of a novel pressurized multistage
565 ammonia production system for hydrogen storage purposes. J. Cleaner Prod. 2018;196:390-9.
566 https://doi.org/10.1016/j.jclepro.2018.06.022
567 [40] Hasan A, Dincer I. Development of an integrated wind and PV system for ammonia and power
568 production for a sustainable community. J. Cleaner Prod. 2019;231:1515-25.
569 https://doi.org/10.1016/j.jclepro.2019.05.110
570 [41] Sánchez A, Martín M. Optimal renewable production of ammonia from water and air. J. Cleaner Prod.
571 2018;178:325-42. https://doi.org/10.1016/j.jclepro.2017.12.279
572 [42] Bicer Y, Dincer I, Zamfirescu C, Vezina G, Raso F. Comparative life cycle assessment of various
573 ammonia production methods. J. Cleaner Prod. 2016;135:1379-95.
574 https://doi.org/10.1016/j.jclepro.2016.07.023
575 [43] Araújo A, Skogestad S. Control structure design for the ammonia synthesis process. Comput. Chem.
576 Eng. 2008;32:2920-32. https://doi.org/10.1016/j.compchemeng.2008.03.001
577 [44] Arora P, Hoadley AFA, Mahajani SM, Ganesh A. Small-scale ammonia production from biomass: A
578 techno-enviro-economic perspective. Ind. Eng. Chem. Res. 2016;55:6422-34.
579 https://doi.org/10.1021/acs.iecr.5b04937
580 [45] Andersson J, Lundgren J. Techno-economic analysis of ammonia production via integrated biomass
581 gasification. Appl. Energy. 2014;130:484-90. https://doi.org/10.1016/j.apenergy.2014.02.029
582 [46] Tripodi A, Compagnoni M, Bahadori E, Rossetti I. Process simulation of ammonia synthesis over
583 optimized Ru/C catalyst and multibed Fe + Ru configurations. J. Ind. Eng. Chem. 2018;66:176-86.
584 https://www.x-mol.com/paperRedirect/684329
585 [47] Yu B-Y, Chien IL. Design and economic evaluation of a coal-based polygeneration process to
586 coproduce synthetic natural gas and ammonia. Ind. Eng. Chem. Res. 2015;54:10073-87.
587 https://doi.org/10.1021/acs.iecr.5b02345
588 [48] Smith AR, Klosek J. A review of air separation technologies and their integration with energy
589 conversion processes. Fuel Process. Technol. 2001;70:115-34. https://doi.org/10.1016/S0378-
590 3820(01)00131-X

[49] Rohr BA, Singh AR, Nørskov JK. A theoretical explanation of the effect of oxygen poisoning on industrial Haber-Bosch catalysts. J. Catal. 2019;372:33-8. https://doi.org/10.1016/j.jcat.2019.01.042
[50] Aspen Technology Inc. Aspen Plus Ammonia Model, http://www.aspentech.com; 2008.
[51] Khademi MH, Sabbaghi RS. Comparison between three types of ammonia synthesis reactor configurations in terms of cooling methods. Chem. Eng. Res. Des. 2017;128:306-17. https://doi.org/10.1016/j.cherd.2017.10.021
[52] Nielsen A, Kjaer J, Hansen B. Rate equation and mechanism of ammonia synthesis at industrial conditions. J. Catal. 1964;3:68-79. https://doi.org/10.1016/0021-9517(64)90094-6
[53] Rossetti I, Pernicone N, Ferrero F, Forni L. Kinetic study of ammonia synthesis on a promoted Ru/C catalyst. Ind. Eng. Chem. Res. 2006;45:4150-5. https://doi.org/10.1021/ie051398g
[54] Nicol W, Hildebrandt D, Glasser D. Crossing reaction equilibrium in an adiabatic reactor system. Dev. Chem. Eng. Miner. Process. 1998;6:41-54. https://doi.org/10.1002/apj.5500060104
[55] Dyson DC, Simon JM. Kinetic expression with diffusion correction for ammonia synthesis on industrial catalyst. Ind. Eng. Chem. Fundam. 1968;7:605-10. https://doi.org/10.1021/i160028a013
[56] Guacci U, Traina F, Ferraris GB, Barisone R. On the application of the Temkin equation in the evaluation of catalysts for the ammonia synthesis. Ind. Eng. Chem. Process Des. Dev. 1977;16:166-76. https://doi.org/10.1021/i260062a002
[57] Temkin M. Kinetics of ammonia synthesis at high pressures. Russ. J. Phys. Chem. A. 1950;24:1312.
[58] Rosowski F, Hornung A, Hinrichsen O, Herein D, Muhler M, Ertl G. Ruthenium catalysts for ammonia synthesis at high pressures: Preparation, characterization, and power-law kinetics. Appl. Catal., A. 1997;151:443-60. https://doi.org/10.1016/S0926-860X(96)00304-3
[59] Hagen S, Barfod R, Fehrmann R, Jacobsen CJH, Teunissen HT, Chorkendorff I. Ammonia synthesis with barium-promoted iron–cobalt alloys supported on carbon. J. Catal. 2003;214:327-35. https://doi.org/10.1016/S0021-9517(02)00182-3
[60] Buzzi Ferraris G, Donati G, Rejna F, Carrà S. An investigation on kinetic models for ammonia synthesis. Chem. Eng. Sci. 1974;29:1621-7. https://doi.org/10.1016/0009-2509(74)87013-2
[61] Gillespie LJ, Beattie JA. The thermodynamic treatment of chemical equilibria in systems composed of real gases. I. An approximate equation for the mass action function applied to the existing data on the Haber equilibrium. Phys. Rev. 1930;36:743-53. https://doi.org/10.1103/PhysRev.36.743
[62] Shaw HR, Wones DR. Fugacity coefficients for hydrogen gas between O degrees and 1000 degrees C, for pressures to 3000 atm. Am. J. Sci. 1964;262:918-29. https://doi.org/10.2475/ajs.262.7.918
[63] Newton RH. Activity coefficients of gases. Ind. Eng. Chem. 1935;27:302-6. https://doi.org/10.1007/978-3-319-46401-5_37
[64] Ashby M. Material and process charts: The CES EduPack Resource Booklet 2; 2009.
[65] Committee of Stainless Steel Producer, AI&SI. Stainless steel in ammonia production. 1978.
[66] U.S. Energy Information Administration. Electric power monthly with data for June 2020,

627 https://www.eia.gov/electricity/monthly/; 2020 [accessed 31 August 2020].
628 [67] Peters MS, Timmerhaus KD, West RE. Plant Design and Economics for Chemical Engineers: 5th ed:
629 McGraw-Hill Science Engineering; 2003.
630 [68] Grosu Y, Faik A, Ortega-Fernández I, D'Aguanno B. Natural magnetite for thermal energy storage:
631 Excellent thermophysical properties, reversible latent heat transition and controlled thermal conductivity.
632 Sol. Energy Mater. Sol. Cells. 2017;161:170-6. https://doi.org/10.1016/j.solmat.2016.12.006
633 [69] Umicore. Ruthenium, https://pmm.umicore.com/en/prices/ruthenium/; 2020 [accessed 31 August
634 2020].
635 [70] Graphene-info. NanoXplore plans a 10,000 ton graphene powder facility, https://www.graphene-
636 info.com/nanoxplore-plans-10000-ton-graphene-powder-facility; 2020 [accessed 31 August 2020].
637 [71] Rossetti I, Forni L. Effect of Ru loading and of Ru precursor in Ru/C catalysts for ammonia synthesis.
638 Appl. Catal., A. 2005;282:315-20. https://doi.org/10.1016/j.apcata.2004.12.024
639 [72] International Renewable Energy Agency. Renewable Power Generation Costs in 2019,
640 https://www.irena.org/publications/2020/Jun/Renewable-Power-Costs-in-2019; 2020 [accessed 31 August
641 2020].
642 [73] Smith C, Hill AK, Torrente-Murciano L. Current and future role of Haber–Bosch ammonia in a carbon-
643 free energy landscape. Energy Environ. Sci. 2020;13:331-44. https://doi.org/10.1039/C9EE02873K
644 [74] Palys M, McCormick A, Cussler E, Daoutidis P. Modeling and optimal design of absorbent enhanced
645 ammonia synthesis. Processes. 2018;6:91. https://doi.org/10.3390/pr6070091
646 [75] Gao W, Wang P, Guo J, Chang F, He T, Wang Q, et al. Barium hydride-mediated nitrogen transfer and
647 hydrogenation for ammonia synthesis: A case study of cobalt. ACS Catal. 2017;7:3654-61.
648 https://doi.org/10.1021/acscatal.7b00284
649 [76] Ye TN, Park SW, Lu Y, Li J, Sasase M, Kitano M, et al. Contribution of nitrogen vacancies to ammonia
650 synthesis over metal nitride catalysts. J. Am. Chem. Soc. 2020;142:14374-83.
651 https://doi.org/10.1021/jacs.0c06624
652 [77] Inoue Y, Kitano M, Tokunari M, Taniguchi T, Ooya K, Abe H, et al. Direct activation of cobalt catalyst
653 by $12CaO{\cdot}7Al_2O_3$ electride for ammonia synthesis. ACS Catal. 2019;9:1670-9.
654 https://doi.org/10.1021/acscatal.8b03650
655 [78] Sato K, Miyahara SI, Ogura Y, Tsujimaru K, Wada Y, Toriyama T, et al. Surface dynamics for creating
656 highly active Ru sites for ammonia synthesis: Accumulation of a low-crystalline, oxygen-deficient
657 nanofraction. ACS Sustainable Chem. Eng. 2020;8:2726-34.
658 https://doi.org/10.1021/acssuschemeng.9b06299
659

# Supplementary Information

**Economies of scale in ammonia synthesis loops embedded with iron- and ruthenium-based catalysts**

Masaki Yoshida†, Takaya Ogawa†*, Yoko Imamura, Keiichi N. Ishihara

Graduate School of Energy Science, Kyoto University, Yoshida-honmachi, Sakyo-ku, Kyoto 606-8501, Japan

†Equal contribution

*Corresponding author: ogawa.takaya.8s@kyoto-u.ac.jp

## A. Explains and results of the ammonia synthesis loop simulation in Aspen Plus©

Aspen Plus© was employed to simulate the whole processes in the loop of ammonia synthesis. The process was based on the template of an ammonia synthesis plant in Aspen Plus© with some modification (Fig. 2) [50]. The RKS-BM (Redlich-Kwong-Soave with Boston-Mathias modification) property method was chosen for the description of the thermodynamic properties of the high-temperature, high-pressure conditions in ammonia synthesis loops. The physical properties were taken from the database in Aspen Plus©. An explanation of the overall process and the assumptions put in this simulation is as follows (Figure A.1, and Table A.1, A.2):

1. It was assumed that the nitrogen feedstock gas was obtained by a cryogenic air separation process supplying the same amount of nitrogen [13, 48].
2. The feedstock consisted of hydrogen and nitrogen in a molar ratio of 3:1, and the pressure was raised by a centrifugal compressor from 1 atm to the reaction pressure.
3. The feedstock was mixed with the reactant gases in the ammonia synthesis loop and fed into the synthesis process (Figure A.1.c).
4. The syngas is cooled to room temperature by preheating the reactant gas and cooling with water and then fed to the refrigeration process (Figure A.1.a and A.1.d).
5. Liquid ammonia and the unreacted gas are separated by refrigeration, and the gas is reused in an ammonia synthesis loop. In some cases, liquid ammonia is used as a refrigerant for the separation of ammonia then recovered (Figure A.1.b).
6. The pressure drop in reactors and heat exchangers was set to zero for simplicity.

In this study, the loops with Fe (KM1R) and Ru/C catalysts as catalysts for ammonia synthesis were simulated, respectively [52, 53]. The reaction conditions depend on the different catalysts. For the Fe catalyst, two types of simulations were performed at reactor temperatures of 400-490°C, 300 bar and

150 bar. On the other hand, the Ru/C catalyst was simulated at 370-460°C in the reactor at 100 bar and 50 bar [52, 53].

Differences in pressure affect the process because the cooling temperature required for ammonia separation is dependent on the loop pressure. The Fe-300bar process (Fig. A.1.a) differs from the other processes in the refrigeration part, where the Fe-300bar process involves only liquid nitrogen cooling for ammonia separation. Figure A.1.d shows the details of the "REFRIG1" block in the main flowsheet of the other processes (Fig. A.1.b). In the "REFRIG1" block, the ammonia gas in the synthesis loop is liquefied by evaporation of liquid nitrogen, liquid oxygen, and pressure-released $NH_3$ product.

Table A.1 shows the summary of the stream results in a simulation of a 100 tonne/day plant for Fe and Ru/C. Also, Table A.2 provides a summary of the results for the blocks (equipment) for all types of loops at the scale of 100 tonne/day. In this study, the plant scale, i.e., the flow rate of the product ammonia, was varied from 0.1 tonne/day to 1000 tonne/day. In the Aspen Plus© simulations, extensive variables such as streamflow rate, reactor volume, heat exchanger area, and compressor rated power varied equally as the plant scale changed. For example, when the product ammonia flow rate increased by a factor of 10, these extensive variables also increased by a factor of 10. On the other hand, intensive variables such as temperature, pressure and molar ratio remained constant as the plant scale changed.

(Continued)

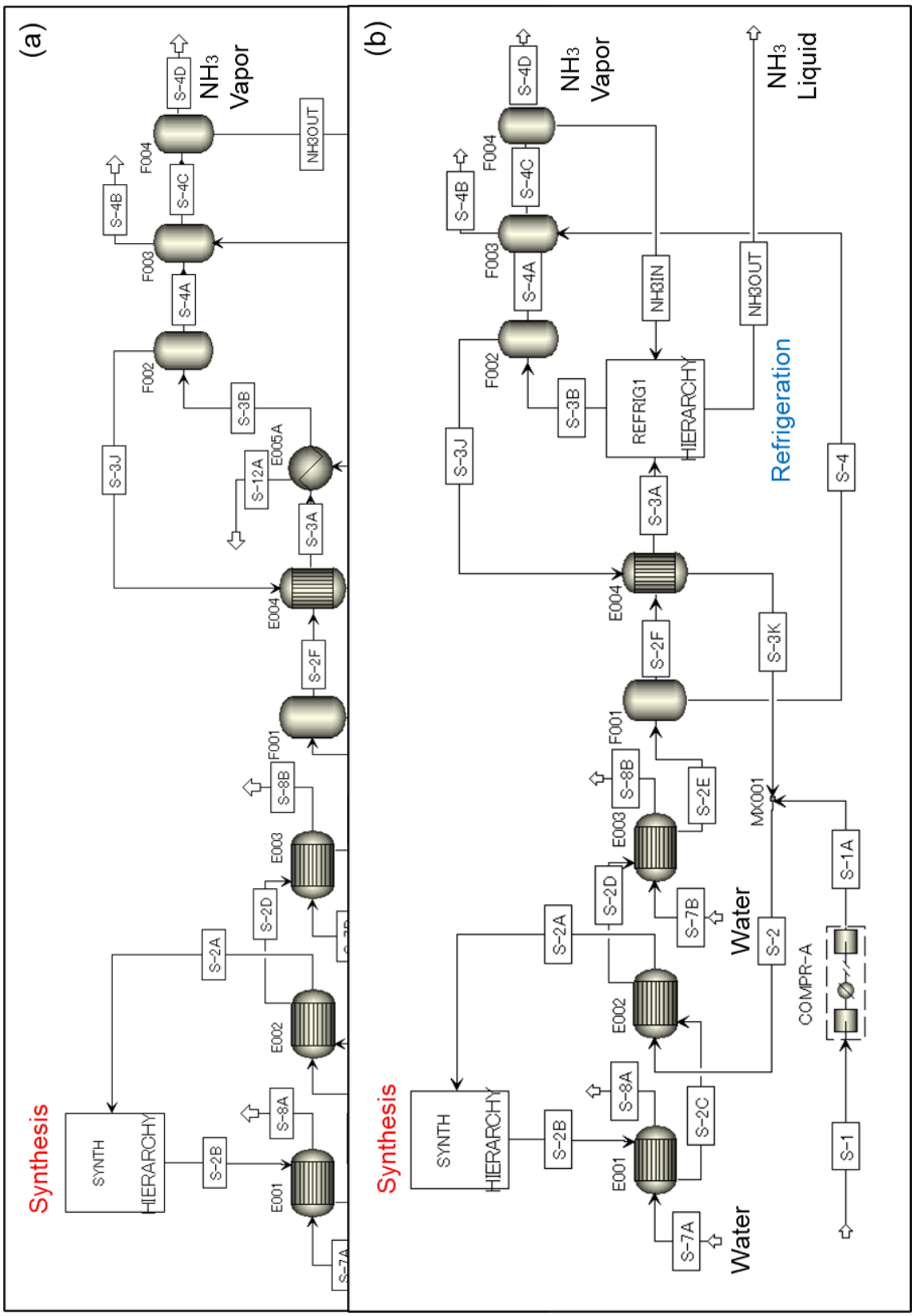
(a)
Synthesis
SYNTH
HIERARCHY
S-2B
S-8A
E001
S-7A
S-2A
E002
S-2D
E003
S-8B
F001
S-2F
E004
S-3A
E005A
S-12A
S-3B
F002
S-3J
S-4A
F003
S-4B
S-4C
F004
S-4D
NH3OUT
NH3 Vapor
(b)
Synthesis
SYNTH
HIERARCHY
S-2B
S-8A
E001
S-7A
Water
S-2C
S-2A
E002
S-2D
E003
S-8B
F001
S-2F
E004
S-3A
S-3J
S-3B
F002
S-4A
F003
S-4B
S-4C
F004
S-4D
NH3 Vapor
REFRIG1
HIERARCHY
NH3IN
NH3OUT
NH3 Liquid
Refrigeration
S-4
S-3K
S-2E
S-7B
Water
MX001
S-2
COMPR-A
S-1A
S-1

711

712

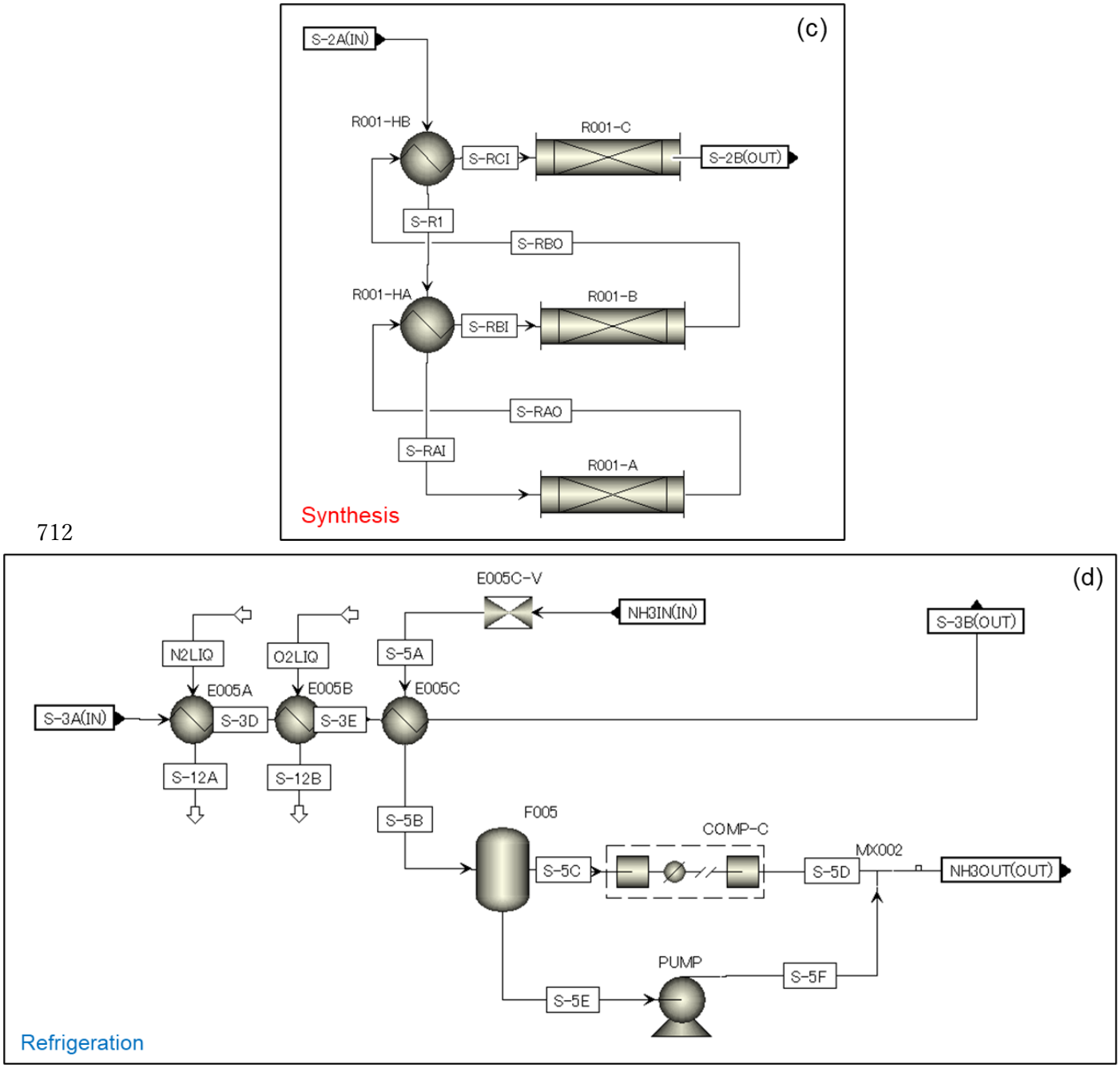


713

714 Fig. A.1. (a) Overall layout of the ammonia synthesis loop simulation in Fe-300bar. (b) Overall layout
715 of the ammonia synthesis plant simulation in Fe-150bar, Ru/C-100bar, Ru/C-75bar and Ru/C-50bar.
716 (c) Flowsheet of the ammonia synthesis process, the details of the “SYNTH” block in the main
717 flowsheet A.1.b. (d) Flowsheet of the ammonia refrigeration process for separation of the product NH3,
718 the details of the “REFRIG1” block in the main flowsheet A.1.b.

719

720 Table A.1. Summary of the stream results in the simulation at the scale of 100 tonne/day
721 ammonia production.

| Fe-300bar | | | | | | | | |
|---|---|---|---|---|---|---|---|---|
| Process | Stream ID | Phase | Temperature °C | Pressure bar | Molar flow rate $10^5$ mol/hr | $H_2$ | $N_2$ | $NH_3$ |
| | | | | | | mole fraction | | |
| Main Flowsheet | **NH3OUT** | **L** | **30.3** | **20** | **2.447** | **0.001** | **0.000** | **0.999** |
| | **S-1** | **V** | **33.0** | **1** | **5.033** | **0.750** | **0.250** | **0.000** |
| | S-1A | V | 30.0 | 300 | 5.033 | 0.750 | 0.250 | 0.000 |
| | S-2 | V | 26.4 | 300 | 16.896 | 0.734 | 0.236 | 0.030 |
| | S-2A | V | 223.0 | 300 | 16.896 | 0.734 | 0.236 | 0.030 |
| | S-2B | V | 487.4 | 300 | 14.408 | 0.602 | 0.190 | 0.208 |
| | S-2C | V | 300.0 | 300 | 14.408 | 0.602 | 0.190 | 0.208 |
| | S-2D | V | 92.3 | 300 | 14.408 | 0.602 | 0.190 | 0.208 |
| | S-2E | L+V | 30.0 | 300 | 14.408 | 0.602 | 0.190 | 0.208 |
| | S-2F | V | 30.0 | 300 | 12.257 | 0.704 | 0.223 | 0.073 |
| | S-3A | L+V | 23.6 | 300 | 12.257 | 0.704 | 0.223 | 0.073 |
| | S-3B | L+V | 11.5 | 300 | 12.257 | 0.704 | 0.223 | 0.073 |
| | S-3J | V | 11.5 | 300 | 11.863 | 0.727 | 0.230 | 0.043 |
| | S-3K | V | 25.0 | 300 | 11.863 | 0.727 | 0.230 | 0.043 |
| | S-4 | L | 30.0 | 300 | 2.151 | 0.017 | 0.006 | 0.976 |
| | S-4A | L | 11.5 | 300 | 0.394 | 0.012 | 0.004 | 0.984 |
| | S-4B | V | 30.5 | 30 | 0.092 | 0.423 | 0.146 | 0.431 |
| | S-4C | L | 30.5 | 30 | 2.453 | 0.001 | 0.001 | 0.998 |
| | S-4D | V | 30.3 | 20 | 0.007 | 0.276 | 0.107 | 0.617 |
| | N2LIQ | L | -196.0 | 1 | 1.258 | 0.000 | 1.000 | 0.000 |
| | S-12A | V | -149.6 | 1 | 1.258 | 0.000 | 1.000 | 0.000 |
| SYNTH | S-2A | V | 223.0 | 300 | 16.896 | 0.734 | 0.236 | 0.030 |
| | S-2B | V | 487.4 | 300 | 14.408 | 0.602 | 0.190 | 0.208 |
| | S-R1 | V | 310.8 | 300 | 16.896 | 0.734 | 0.236 | 0.030 |
| | S-RAI | V | 400.0 | 300 | 16.896 | 0.734 | 0.236 | 0.030 |
| | S-RAO | V | 490.0 | 300 | 16.042 | 0.693 | 0.222 | 0.085 |
| | S-RBI | V | 400.0 | 300 | 16.042 | 0.693 | 0.222 | 0.085 |
| | S-RBO | V | 489.9 | 300 | 15.206 | 0.649 | 0.207 | 0.145 |
| | S-RCI | V | 400.0 | 300 | 15.206 | 0.649 | 0.207 | 0.145 |

722 (Continued)
723

| Fe-150bar | | | | | | | | |
|---|---|---|---|---|---|---|---|---|
| Process | Stream ID | Phase | Temperature °C | Pressure bar | Molar flow rate $10^5$ mol/hr | $H_2$ mole fraction | $N_2$ | $NH_3$ |
| Main Flowsheet | **NH3IN** | **L** | **16.3** | **20** | **2.499** | **0.001** | **0.000** | **0.999** |
| | **NH3OUT** | **L+V** | **4.8** | **20** | **2.499** | **0.001** | **0.000** | **0.999** |
| | **S-1** | **V** | **33.0** | **1** | **5.033** | **0.750** | **0.250** | **0.000** |
| | S-1A | V | 30.0 | 150 | 5.033 | 0.750 | 0.250 | 0.000 |
| | S-2 | V | 26.2 | 150 | 20.501 | 0.739 | 0.231 | 0.030 |
| | S-2A | V | 223.0 | 150 | 20.501 | 0.739 | 0.231 | 0.030 |
| | S-2B | V | 439.6 | 150 | 17.998 | 0.633 | 0.194 | 0.174 |
| | S-2C | V | 300.0 | 150 | 17.998 | 0.633 | 0.194 | 0.174 |
| | S-2D | V | 91.5 | 150 | 17.998 | 0.633 | 0.194 | 0.174 |
| | S-2E | L+V | 30.0 | 150 | 17.998 | 0.633 | 0.194 | 0.174 |
| | S-2F | V | 30.0 | 150 | 16.747 | 0.679 | 0.208 | 0.113 |
| | S-3A | L+V | 21.1 | 150 | 16.747 | 0.679 | 0.208 | 0.113 |
| | S-3B | L+V | -2.7 | 150 | 16.747 | 0.679 | 0.208 | 0.113 |
| | S-3J | V | -2.7 | 150 | 15.468 | 0.735 | 0.225 | 0.040 |
| | S-3K | V | 25.0 | 150 | 15.468 | 0.735 | 0.225 | 0.040 |
| | S-4 | L | 30.0 | 150 | 1.252 | 0.010 | 0.003 | 0.987 |
| | S-4A | L | -2.7 | 150 | 1.279 | 0.005 | 0.002 | 0.993 |
| | S-4B | V | 16.2 | 30 | 0.028 | 0.533 | 0.187 | 0.280 |
| | S-4C | L | 16.2 | 30 | 2.503 | 0.001 | 0.001 | 0.998 |
| | S-4D | V | 16.3 | 20 | 0.003 | 0.426 | 0.166 | 0.408 |

724 (Continued

725

| Fe-150bar | | | | | | | | |
|---|---|---|---|---|---|---|---|---|
| Process | Stream ID | Phase | Temperature °C | Pressure bar | Molar flow rate $10^5$ mol/hr | $H_2$ mole fraction | $N_2$ | $NH_3$ |
| SYNTH | S-2A | V | 223.0 | 150 | 20.501 | 0.739 | 0.231 | 0.030 |
| | S-2B | V | 439.6 | 150 | 17.998 | 0.633 | 0.194 | 0.174 |
| | S-R1 | V | 311.0 | 150 | 20.501 | 0.739 | 0.231 | 0.030 |
| | S-RAI | V | 400.0 | 150 | 20.502 | 0.739 | 0.231 | 0.030 |
| | S-RAO | V | 490.0 | 150 | 19.461 | 0.698 | 0.217 | 0.085 |
| | S-RBI | V | 400.0 | 150 | 19.461 | 0.698 | 0.217 | 0.085 |
| | S-RBO | V | 490.0 | 150 | 18.440 | 0.654 | 0.201 | 0.145 |
| | S-RCI | V | 400.0 | 150 | 18.440 | 0.654 | 0.201 | 0.145 |
| REFRIG1 | NH3IN | L | 16.3 | 20 | 2.499 | 0.001 | 0.000 | 0.999 |
| | NH3OUT | L+V | 4.8 | 20 | 2.499 | 0.001 | 0.000 | 0.999 |
| | N2LIQ | L | -196.0 | 1 | 1.258 | 0.000 | 1.000 | 0.000 |
| | O2LIQ | L | -196.0 | 1 | 0.339 | 0.000 | 0.000 | 0.000 |
| | S-12A | V | 8.7 | 1 | 1.258 | 0.000 | 1.000 | 0.000 |
| | S-12B | V | 4.9 | 1 | 0.339 | 0.000 | 0.000 | 0.000 |
| | S-3A | L+V | 21.1 | 150 | 16.746 | 0.679 | 0.208 | 0.113 |
| | S-3B | L+V | -2.7 | 150 | 16.747 | 0.679 | 0.208 | 0.113 |
| | S-3D | L+V | 9.7 | 150 | 16.746 | 0.679 | 0.208 | 0.113 |
| | S-3E | L+V | 5.9 | 150 | 16.746 | 0.679 | 0.208 | 0.113 |
| | S-5A | L+V | -3.1 | 4 | 2.499 | 0.001 | 0.000 | 0.999 |
| | S-5B | L+V | -2.8 | 4 | 2.499 | 0.001 | 0.000 | 0.999 |
| | S-5C | V | -2.8 | 4 | 0.616 | 0.003 | 0.001 | 0.996 |
| | S-5D | L+V | 25.0 | 20 | 0.616 | 0.003 | 0.001 | 0.996 |
| | S-5E | L | -2.8 | 4 | 1.883 | 0.000 | 0.000 | 1.000 |
| | S-5F | L | -2.1 | 20 | 1.883 | 0.000 | 0.000 | 1.000 |

726 (Continued))

727

| Ru/C-100bar | | | | | | | | |
|---|---|---|---|---|---|---|---|---|
| Process | Stream ID | Phase | Temperature °C | Pressure bar | Molar flow rate $10^5$ mol/hr | $H_2$ mole fraction | $N_2$ | $NH_3$ |
| Main Flowsheet | **NH3IN** | **L** | **-1.7** | **20** | **2.513** | **0.001** | **0.000** | **0.999** |
| | **NH3OUT** | **L** | **9.9** | **20** | **2.513** | **0.001** | **0.000** | **0.999** |
| | **S-1** | **V** | **33.0** | **1** | **5.033** | **0.750** | **0.250** | **0.000** |
| | S-1A | V | 30.0 | 100 | 5.033 | 0.750 | 0.250 | 0.000 |
| | S-2 | V | 26.2 | 100 | 20.803 | 0.727 | 0.243 | 0.030 |
| | S-2A | V | 193.0 | 100 | 20.803 | 0.727 | 0.243 | 0.030 |
| | S-2B | V | 405.9 | 100 | 18.293 | 0.620 | 0.208 | 0.172 |
| | S-2C | V | 300.0 | 100 | 18.293 | 0.620 | 0.208 | 0.172 |
| | S-2D | V | 122.8 | 100 | 18.293 | 0.620 | 0.208 | 0.172 |
| | S-2E | L+V | 30.0 | 100 | 18.293 | 0.620 | 0.208 | 0.172 |
| | S-2F | V | 30.0 | 100 | 17.887 | 0.634 | 0.213 | 0.153 |
| | S-3A | L+V | 21.8 | 100 | 17.887 | 0.634 | 0.213 | 0.153 |
| | S-3B | L+V | -10.5 | 100 | 17.887 | 0.634 | 0.213 | 0.153 |
| | S-3J | V | -10.5 | 100 | 15.770 | 0.719 | 0.241 | 0.040 |
| | S-3K | V | 25.0 | 100 | 15.770 | 0.719 | 0.241 | 0.040 |
| | S-4 | L | 30.0 | 100 | 0.407 | 0.006 | 0.003 | 0.991 |
| | S-4A | L | -10.5 | 100 | 2.117 | 0.003 | 0.001 | 0.996 |
| | S-4B | V | -1.9 | 30 | 0.010 | 0.610 | 0.239 | 0.150 |
| | S-4C | L | -1.9 | 30 | 2.515 | 0.001 | 0.000 | 0.999 |
| | S-4D | V | -1.7 | 20 | 0.002 | 0.543 | 0.237 | 0.220 |

728 (Continued)

729

| Ru/C-100bar | | | | | | | | |
|---|---|---|---|---|---|---|---|---|
| Process | Stream ID | Phase | Temperature °C | Pressure bar | Molar flow rate $10^5$ mol/hr | $H_2$ | $N_2$ | $NH_3$ |
| | | | | | | mole fraction | | |
| SYNTH | S-2A | V | 193.0 | 100 | 20.803 | 0.727 | 0.243 | 0.030 |
| | S-2B | V | 405.9 | 100 | 18.293 | 0.620 | 0.208 | 0.172 |
| | S-R1 | V | 280.7 | 100 | 20.803 | 0.727 | 0.243 | 0.030 |
| | S-RAI | V | 370.0 | 100 | 20.805 | 0.727 | 0.243 | 0.030 |
| | S-RAO | V | 460.0 | 100 | 19.743 | 0.685 | 0.229 | 0.086 |
| | S-RBI | V | 370.0 | 100 | 19.743 | 0.685 | 0.229 | 0.086 |
| | S-RBO | V | 460.0 | 100 | 18.703 | 0.640 | 0.214 | 0.146 |
| | S-RCI | V | 370.0 | 100 | 18.703 | 0.640 | 0.214 | 0.146 |
| REFRIG1 | NH3IN | L | -1.7 | 20 | 2.513 | 0.001 | 0.000 | 0.999 |
| | NH3OUT | L | 9.9 | 20 | 2.513 | 0.001 | 0.000 | 0.999 |
| | N2LIQ | L | -196.0 | 1 | 1.258 | 0.000 | 1.000 | 0.000 |
| | O2LIQ | L | -196.0 | 1 | 0.338 | 0.000 | 0.000 | 0.000 |
| | S-12A | V | 12.5 | 1 | 1.258 | 0.000 | 1.000 | 0.000 |
| | S-12B | V | 9.7 | 1 | 0.338 | 0.000 | 0.000 | 0.000 |
| | S-3A | L+V | 21.8 | 100 | 17.888 | 0.634 | 0.213 | 0.153 |
| | S-3B | L+V | -10.5 | 100 | 17.888 | 0.634 | 0.213 | 0.153 |
| | S-3D | L+V | 13.5 | 100 | 17.888 | 0.634 | 0.213 | 0.153 |
| | S-3E | L+V | 10.7 | 100 | 17.888 | 0.634 | 0.213 | 0.153 |
| | S-5A | L+V | -11.0 | 3 | 2.513 | 0.001 | 0.000 | 0.999 |
| | S-5B | L+V | -10.4 | 3 | 2.513 | 0.001 | 0.000 | 0.999 |
| | S-5C | V | -10.4 | 3 | 1.390 | 0.001 | 0.001 | 0.998 |
| | S-5D | L+V | 25.0 | 20 | 1.390 | 0.001 | 0.001 | 0.998 |
| | S-5E | L | -10.4 | 3 | 1.123 | 0.000 | 0.000 | 1.000 |
| | S-5F | L | -9.7 | 20 | 1.123 | 0.000 | 0.000 | 1.000 |

730 (Continued)

731

732

| Ru/C-100bar | | | | | | | | |
|---|---|---|---|---|---|---|---|---|
| Process | Stream | | Temperature | Pressure | Molar flow rate | $H_2$ | $N_2$ | $NH_3$ |
| | ID | Phase | °C | bar | $10^5$ mol/hr | mole fraction | | |
| SYNTH | S-2A | V | 193.0 | 100 | 20.803 | 0.727 | 0.243 | 0.030 |
| | S-2B | V | 405.9 | 100 | 18.293 | 0.620 | 0.208 | 0.172 |
| | S-R1 | V | 280.7 | 100 | 20.803 | 0.727 | 0.243 | 0.030 |
| | S-RAI | V | 370.0 | 100 | 20.805 | 0.727 | 0.243 | 0.030 |
| | S-RAO | V | 460.0 | 100 | 19.743 | 0.685 | 0.229 | 0.086 |
| | S-RBI | V | 370.0 | 100 | 19.743 | 0.685 | 0.229 | 0.086 |
| | S-RBO | V | 460.0 | 100 | 18.703 | 0.640 | 0.214 | 0.146 |
| | S-RCI | V | 370.0 | 100 | 18.703 | 0.640 | 0.214 | 0.146 |
| REFRIG1 | NH3IN | L | -1.7 | 20 | 2.513 | 0.001 | 0.000 | 0.999 |
| | NH3OUT | L | 9.9 | 20 | 2.513 | 0.001 | 0.000 | 0.999 |
| | N2LIQ | L | -196.0 | 1 | 1.258 | 0.000 | 1.000 | 0.000 |
| | O2LIQ | L | -196.0 | 1 | 0.338 | 0.000 | 0.000 | 0.000 |
| | S-12A | V | 12.5 | 1 | 1.258 | 0.000 | 1.000 | 0.000 |
| | S-12B | V | 9.7 | 1 | 0.338 | 0.000 | 0.000 | 0.000 |
| | S-3A | L+V | 21.8 | 100 | 17.888 | 0.634 | 0.213 | 0.153 |
| | S-3B | L+V | -10.5 | 100 | 17.888 | 0.634 | 0.213 | 0.153 |
| | S-3D | L+V | 13.5 | 100 | 17.888 | 0.634 | 0.213 | 0.153 |
| | S-3E | L+V | 10.7 | 100 | 17.888 | 0.634 | 0.213 | 0.153 |
| | S-5A | L+V | -11.0 | 3 | 2.513 | 0.001 | 0.000 | 0.999 |
| | S-5B | L+V | -10.4 | 3 | 2.513 | 0.001 | 0.000 | 0.999 |
| | S-5C | V | -10.4 | 3 | 1.390 | 0.001 | 0.001 | 0.998 |
| | S-5D | L+V | 25.0 | 20 | 1.390 | 0.001 | 0.001 | 0.998 |
| | S-5E | L | -10.4 | 3 | 1.123 | 0.000 | 0.000 | 1.000 |
| | S-5F | L | -9.7 | 20 | 1.123 | 0.000 | 0.000 | 1.000 |

733 (Continued)

734

| Ru/C-75bar | | | | | | | | |
|---|---|---|---|---|---|---|---|---|
| Process | Stream ID | Phase | Temperature °C | Pressure bar | Molar flow rate $10^5$ mol/hr | $H_2$ mole fraction | $N_2$ | $NH_3$ |
| Main Flowsheet | **NH3IN** | **L** | **-15.9** | **20** | **2.515** | **0.000** | **0.000** | **0.999** |
| | **NH3OUT** | **L** | **14.0** | **20** | **2.515** | **0.000** | **0.000** | **0.999** |
| | **S-1** | **V** | **33.0** | **1** | **5.033** | **0.750** | **0.250** | **0.000** |
| | S-1A | V | 30.0 | 75 | 5.033 | 0.750 | 0.250 | 0.000 |
| | S-2 | V | 26.0 | 75 | 24.975 | 0.719 | 0.251 | 0.030 |
| | S-2A | V | 228.0 | 75 | 24.975 | 0.719 | 0.251 | 0.030 |
| | S-2B | V | 405.1 | 75 | 22.462 | 0.631 | 0.223 | 0.145 |
| | S-2C | V | 300.0 | 75 | 22.462 | 0.631 | 0.223 | 0.145 |
| | S-2D | V | 87.2 | 75 | 22.462 | 0.631 | 0.223 | 0.145 |
| | S-2E | L+V | 30.0 | 75 | 22.462 | 0.631 | 0.223 | 0.145 |
| | S-2F | V | 30.0 | 75 | 22.462 | 0.631 | 0.223 | 0.145 |
| | S-3A | L+V | 13.6 | 75 | 22.462 | 0.631 | 0.223 | 0.145 |
| | S-3B | L+V | -17.5 | 75 | 22.462 | 0.631 | 0.223 | 0.145 |
| | S-3J | V | -17.5 | 75 | 19.942 | 0.711 | 0.251 | 0.038 |
| | S-3K | V | 25.0 | 75 | 19.942 | 0.711 | 0.251 | 0.038 |
| | S-4 | L | na | 75 | 0.000 | na | na | na |
| | S-4A | L | -17.5 | 75 | 2.520 | 0.002 | 0.001 | 0.997 |
| | S-4B | V | -16.2 | 30 | 0.004 | 0.644 | 0.270 | 0.086 |
| | S-4C | L | -16.2 | 30 | 2.516 | 0.001 | 0.000 | 0.999 |
| | S-4D | V | -15.9 | 20 | 0.001 | 0.595 | 0.279 | 0.126 |

735 (Continued)

736

737

| Ru/C-75bar | | | | | | | | |
|---|---|---|---|---|---|---|---|---|
| Process | Stream ID | Phase | Temperature °C | Pressure bar | Molar flow rate $10^5$ mol/hr | $H_2$ mole fraction | $N_2$ | $NH_3$ |
| SYNTH | S-2A | V | 228.0 | 75 | 24.975 | 0.719 | 0.251 | 0.030 |
| | S-2B | V | 405.1 | 75 | 22.462 | 0.631 | 0.223 | 0.145 |
| | S-R1 | V | 280.7 | 75 | 24.975 | 0.719 | 0.251 | 0.030 |
| | S-RAI | V | 370.0 | 75 | 24.975 | 0.719 | 0.251 | 0.030 |
| | S-RAO | V | 460.0 | 75 | 23.699 | 0.677 | 0.238 | 0.085 |
| | S-RBI | V | 370.0 | 75 | 23.699 | 0.677 | 0.238 | 0.085 |
| | S-RBO | V | 423.8 | 75 | 22.947 | 0.650 | 0.229 | 0.121 |
| | S-RCI | V | 370.0 | 75 | 22.947 | 0.650 | 0.229 | 0.121 |
| REFRIG1 | NH3IN | L | -15.9 | 20 | 2.514 | 0.000 | 0.000 | 0.999 |
| | NH3OUT | L | 14.0 | 20 | 2.514 | 0.000 | 0.000 | 0.999 |
| | N2LIQ | L | -196.0 | 1 | 1.259 | 0.000 | 1.000 | 0.000 |
| | O2LIQ | L | -196.0 | 1 | 0.339 | 0.000 | 0.000 | 0.000 |
| | S-12A | V | 6.5 | 1 | 1.259 | 0.000 | 1.000 | 0.000 |
| | S-12B | V | 4.5 | 1 | 0.339 | 0.000 | 0.000 | 0.000 |
| | S-3A | L+V | 13.6 | 75 | 22.463 | 0.631 | 0.223 | 0.145 |
| | S-3B | L+V | -17.5 | 75 | 22.462 | 0.631 | 0.223 | 0.145 |
| | S-3D | L+V | 7.5 | 75 | 22.463 | 0.631 | 0.223 | 0.145 |
| | S-3E | L+V | 5.5 | 75 | 22.463 | 0.631 | 0.223 | 0.145 |
| | S-5A | L+V | -20.2 | 2 | 2.514 | 0.000 | 0.000 | 0.999 |
| | S-5B | L+V | -19.2 | 2 | 2.514 | 0.000 | 0.000 | 0.999 |
| | S-5C | V | -19.2 | 2 | 1.858 | 0.001 | 0.000 | 0.999 |
| | S-5D | L+V | 25.0 | 20 | 1.858 | 0.001 | 0.000 | 0.999 |
| | S-5E | L | -19.2 | 2 | 0.656 | 0.000 | 0.000 | 1.000 |
| | S-5F | L | -18.5 | 20 | 0.656 | 0.000 | 0.000 | 1.000 |

738 (Continued)

739

740

| Ru/C-50bar | | | | | | | | |
|---|---|---|---|---|---|---|---|---|
| Process | Stream ID | Phase | Temperature °C | Pressure bar | Molar flow rate $10^5$ mol/hr | $H_2$ mole fraction | $N_2$ | $NH_3$ |
| Main Flowsheet | **NH3IN** | **L** | **-25.1** | **20** | **2.519** | **0.000** | **0.000** | **0.999** |
| | **NH3OUT** | **L** | **15.4** | **20** | **2.519** | **0.000** | **0.000** | **0.999** |
| | **S-1** | **V** | **33.0** | **1** | **5.033** | **0.750** | **0.250** | **0.000** |
| | S-1A | V | 30.0 | 50 | 5.033 | 0.750 | 0.250 | 0.000 |
| | S-2 | V | 25.8 | 50 | 31.506 | 0.727 | 0.243 | 0.030 |
| | S-2A | V | 257.0 | 50 | 31.506 | 0.727 | 0.243 | 0.030 |
| | S-2B | V | 396.9 | 50 | 28.990 | 0.660 | 0.220 | 0.120 |
| | S-2C | V | 300.0 | 50 | 28.990 | 0.660 | 0.220 | 0.120 |
| | S-2D | V | 58.6 | 50 | 28.990 | 0.660 | 0.220 | 0.120 |
| | S-2E | V | 30.0 | 50 | 28.990 | 0.660 | 0.220 | 0.120 |
| | S-2F | V | 30.0 | 50 | 28.992 | 0.660 | 0.220 | 0.120 |
| | S-3A | L+V | -0.7 | 50 | 28.992 | 0.660 | 0.220 | 0.120 |
| | S-3B | L+V | -26.0 | 50 | 28.994 | 0.660 | 0.220 | 0.120 |
| | S-3J | V | -26.0 | 50 | 26.473 | 0.723 | 0.241 | 0.036 |
| | S-3K | V | 25.0 | 50 | 26.473 | 0.723 | 0.241 | 0.036 |
| | S-4 | L+V | na | 50 | 0.000 | na | na | na |
| | S-4A | L | -26.0 | 50 | 2.522 | 0.001 | 0.000 | 0.999 |
| | S-4B | V | -25.4 | 30 | 0.001 | 0.683 | 0.259 | 0.057 |
| | S-4C | L | -25.4 | 30 | 2.520 | 0.001 | 0.000 | 0.999 |
| | S-4D | V | -25.1 | 20 | 0.001 | 0.641 | 0.275 | 0.084 |

741 (Continued)

742

| Ru/C-50bar | | | | | | | | |
|---|---|---|---|---|---|---|---|---|
| Process | Stream ID | Phase | Temperature °C | Pressure bar | Molar flow rate $10^5$ mol/hr | $H_2$ | $N_2$ mole fraction | $NH_3$ |
| SYNTH | S-2A | V | 257.0 | 50 | 31.506 | 0.727 | 0.243 | 0.030 |
| | S-2B | V | 396.9 | 50 | 28.990 | 0.660 | 0.220 | 0.120 |
| | S-R1 | V | 304.1 | 50 | 31.506 | 0.727 | 0.243 | 0.030 |
| | S-RAI | V | 370.0 | 50 | 31.507 | 0.727 | 0.243 | 0.030 |
| | S-RAO | V | 436.5 | 50 | 30.313 | 0.697 | 0.233 | 0.071 |
| | S-RBI | V | 370.0 | 50 | 30.313 | 0.697 | 0.233 | 0.071 |
| | S-RBO | V | 417.9 | 50 | 29.464 | 0.674 | 0.225 | 0.102 |
| | S-RCI | V | 370.0 | 50 | 29.464 | 0.674 | 0.225 | 0.102 |
| REFRIG1 | NH3IN | L | -25.1 | 20 | 2.519 | 0.000 | 0.000 | 0.999 |
| | NH3OUT | L | 15.4 | 20 | 2.519 | 0.000 | 0.000 | 0.999 |
| | N2LIQ | L | -196.0 | 1 | 1.258 | 0.000 | 1.000 | 0.000 |
| | O2LIQ | L | -196.0 | 1 | 0.339 | 0.000 | 0.000 | 0.000 |
| | S-12A | V | -6.2 | 1 | 1.258 | 0.000 | 1.000 | 0.000 |
| | S-12B | V | -7.7 | 1 | 0.339 | 0.000 | 0.000 | 0.000 |
| | S-3A | L+V | -0.7 | 50 | 28.993 | 0.660 | 0.220 | 0.120 |
| | S-3B | L+V | -26.0 | 50 | 28.995 | 0.660 | 0.220 | 0.120 |
| | S-3D | L+V | -5.2 | 50 | 28.993 | 0.660 | 0.220 | 0.120 |
| | S-3E | L+V | -6.7 | 50 | 28.993 | 0.660 | 0.220 | 0.120 |
| | S-5A | L+V | -27.1 | 2 | 2.519 | 0.000 | 0.000 | 0.999 |
| | S-5B | L+V | -25.7 | 2 | 2.519 | 0.000 | 0.000 | 0.999 |
| | S-5C | V | -25.7 | 2 | 2.014 | 0.000 | 0.000 | 0.999 |
| | S-5D | L | 25.0 | 20 | 2.014 | 0.000 | 0.000 | 0.999 |
| | S-5E | L | -25.7 | 2 | 0.506 | 0.000 | 0.000 | 1.000 |
| | S-5F | L | -25.0 | 20 | 0.506 | 0.000 | 0.000 | 1.000 |

743

744

745 Table A.2.

746 Summary of the block results in the simulation at the scale of 100 tonne/day ammonia production.

| Equipment | Units | Block-ID | Fe-300bar | Fe-150bar | Ru/C-100bar | Ru/C-75bar | Ru/C-50bar |
|---|---|---|---|---|---|---|---|
| Reactor | $m^3$ | R001-A | 0.139 | 0.609 | 0.825 | 1.200 | 1.784 |
| | | R001-B | 0.344 | 1.887 | 1.711 | 1.721 | 2.689 |
| | | R001-C | 0.673 | 1.721 | 1.418 | 1.849 | 2.578 |
| Total volume | $m^3$ | | 1.155 | 4.217 | 3.954 | 4.770 | 7.050 |
| Heat exchanger | $m^2$ | E001A | 9.088 | 8.598 | 6.790 | 8.237 | 9.882 |
| | | E002 | 47.520 | 56.695 | 33.754 | 74.644 | 189.183 |
| | | E003A | 159.276 | 136.520 | 93.852 | 83.999 | 84.090 |
| | | E004* | 21.110 | 36.283 | 38.440 | 58.941 | 105.582 |
| | | E005A* | 1.535 | 7.004 | 7.567 | 8.185 | 8.864 |
| | | E005B* | null | 2.771 | 2.917 | 3.093 | 3.299 |
| | | E005C* | null | 114.032 | 174.811 | 261.054 | 239.791 |
| | | R001-HB | 16.787 | 20.254 | 20.342 | 24.394 | 30.842 |
| | | R001-HC | 8.347 | 10.030 | 10.088 | 9.072 | 12.835 |
| Total area | $m^2$ | | 263.664 | 392.187 | 388.561 | 531.620 | 684.368 |
| Compressor | MW | COMPR-A | 3.552 | 3.000 | 2.702 | 2.499 | 2.224 |
| | MW | COMPR-B* | null | 0.101 | 0.274 | 0.412 | 0.552 |
| Pump | kW | PUMP* | null | 4.253 | 2.652 | 1.624 | 1.254 |
| Total rated power | MW | | 3.552 | 3.105 | 2.978 | 2.913 | 2.777 |

747 * Blocks we defined as used for ammonia separation.

748

## B. Explains and results of the cost evaluation of the ammonia synthesis loop

In this study, the pump, the block “PUMP” in the simulation, was excluded from the cost evaluation because the capital cost of pumps relative to the capital cost of compressors was negligible [10] and the rated power of the pump was at most 0.14 % of the total rated power in the all processes (Table A.2).

Two types of parameters were used to determine the capital cost of the compressor, “Low” and “High,” depending on the rated power of the compressor [10]. Since these two capital costs are intersected by approximately 8,000 kW of rated power (Fig B.1), 8,000 kW was set as the criterion for choosing between the two types of parameters.

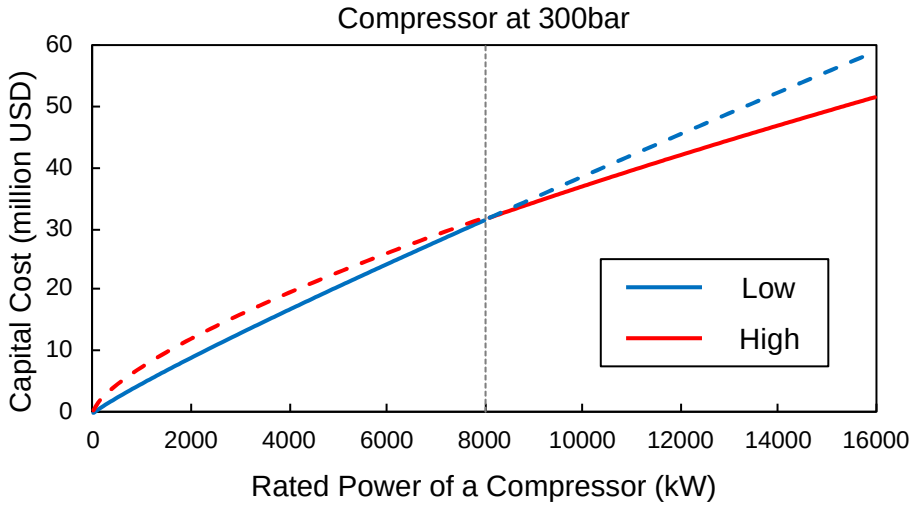


Fig. B.1. The capital cost of a compressor by two types of parameters.

Table B.1 shows the sum of the basis of equipment, the total capital cost by equipment type, the operation cost and the total cost of the ammonia synthesis loop. Tables B.2 represents the summary of the breakdown of the total loop cost on different scales. Table B.3 indicates the total cost for ammonia separation, including heat exchanger, compressor, and power consumption for the compressor in the separation process (Table A.3).

767 Table B.1. Breakdown of the cost of ammonia synthesis loop at the scale of 100 tonne/day.

| | | Unit | Fe-300bar | Fe-150bar | Ru/C-100bar | Ru/C-75bar | Ru/C-50bar |
|---|---|---|---|---|---|---|---|
| Reactor | Total volume | $m^3$ | 1.155 | 4.217 | 3.954 | 4.770 | 7.050 |
| | Total cost | million USD | 1.063 | 1.166 | 0.816 | 0.773 | 0.778 |
| Catalyst | Total weight | tonne | 3.234 | 11.806 | 3.163 | 3.816 | 5.640 |
| | Total cost | million USD | 0.001 | 0.004 | 2.031 | 1.925 | 3.621 |
| Heat exchanger | Total area | | 263.7 | 392.2 | 388.6 | 388.9 | 684.4 |
| | Total cost | million USD | 1.148 | 1.622 | 1.588 | 2.450 | 2.309 |
| Compressor | Total rated power | MW | 3.552 | 3.101 | 2.976 | 2.978 | 2.776 |
| | Total cost | million USD | 15.176 | 13.657 | 13.382 | 13.249 | 12.803 |
| Power | Total rated power | MW | 3.552 | 3.105 | 2.978 | 2.981 | 2.777 |
| | Total cost | million USD | 34.687 | 30.282 | 29.061 | 28.431 | 27.107 |
| Total cost of ammonia synthesis loop | | million USD | 52.075 | 46.731 | 46.878 | 46.829 | 46.619 |

768

769

770 Table B.2. Summary of the breakdown of the total ammonia synthesis loop cost in
771 different scales.

| Fe-300bar | Scale (tonne/day) | 0.1 | 1 | 10 | 100 | 500 |
|---|---|---|---|---|---|---|
| Reactor | million USD | 0.141 | 0.201 | 0.401 | 1.063 | 2.304 |
| Catalyst | | 0.000 | 0.000 | 0.000 | 0.001 | 0.006 |
| Heat exchanger | | 0.155 | 0.186 | 0.343 | 1.148 | 3.283 |
| Compressor | | 0.035 | 0.245 | 1.914 | 15.176 | 55.625 |
| Power consumption | | 0.035 | 0.347 | 3.469 | 34.687 | 173.434 |
| Total loop cost | | 0.365 | 0.978 | 6.127 | 52.075 | 234.651 |
| Fe-150bar | Scale (tonne/day) | 0.1 | 1 | 10 | 100 | 500 |
| Reactor | million USD | 0.144 | 0.211 | 0.432 | 1.166 | 2.543 |
| Catalyst | | 0.000 | 0.000 | 0.000 | 0.004 | 0.021 |
| Heat exchanger | | 0.159 | 0.204 | 0.435 | 1.622 | 4.770 |
| Compressor | | 0.036 | 0.225 | 1.727 | 13.657 | 51.965 |
| Power consumption | | 0.030 | 0.303 | 3.028 | 30.282 | 151.409 |
| Total loop cost | | 0.368 | 0.942 | 5.623 | 46.731 | 210.708 |
| Ru/C-100bar | Scale (tonne/day) | 0.1 | 1 | 10 | 100 | 500 |
| Reactor | million USD | 0.134 | 0.179 | 0.327 | 0.816 | 1.735 |
| Catalyst | | 0.002 | 0.020 | 0.203 | 2.031 | 10.156 |
| Heat exchanger | | 0.158 | 0.202 | 0.429 | 1.588 | 4.664 |
| Compressor | | 0.035 | 0.220 | 1.692 | 13.382 | 52.247 |
| Power consumption | | 0.029 | 0.291 | 2.906 | 29.061 | 145.305 |
| Total loop cost | | 0.359 | 0.913 | 5.556 | 46.878 | 214.107 |
| Ru/C-75bar | Scale (tonne/day) | 0.1 | 1 | 10 | 100 | 500 |
| Reactor | million USD | 0.133 | 0.175 | 0.314 | 0.773 | 1.636 |
| Catalyst | | 0.002 | 0.024 | 0.245 | 2.450 | 12.250 |
| Heat exchanger | | 0.161 | 0.215 | 0.494 | 1.925 | 5.722 |
| Compressor | | 0.035 | 0.218 | 1.675 | 13.249 | 52.639 |
| Power consumption | | 0.028 | 0.284 | 2.843 | 28.431 | 142.155 |
| Total loop cost | | 0.360 | 0.917 | 5.572 | 46.829 | 214.402 |
| Ru/C-50bar | Scale (tonne/day) | 0.1 | 1 | 10 | 100 | 500 |
| Reactor | million USD | 0.133 | 0.175 | 0.315 | 0.778 | 1.647 |
| Catalyst | | 0.004 | 0.036 | 0.362 | 3.621 | 18.107 |
| Heat exchanger | | 0.164 | 0.230 | 0.569 | 2.309 | 6.926 |

| | | | | | |
|---|---|---|---|---|---|
| Compressor | 0.034 | 0.211 | 1.619 | 12.803 | 51.986 |
| Power consumption | 0.027 | 0.271 | 2.711 | 27.107 | 135.533 |
| Total loop cost | 0.362 | 0.924 | 5.576 | 46.619 | 214.199 |

772

773

774 Table B.3. Total cost for ammonia separation in different scales.

| Fe-300bar | Scale (tonne/day) | 0.1 | 1 | 10 | 100 | 500 |
|---|---|---|---|---|---|---|
| Total loop cost | million USD | 0.365 | 0.978 | 6.127 | 52.075 | 234.651 |
| Cost for separation | | 0.067 | 0.070 | 0.091 | 0.193 | 0.466 |
| Ratio for separation | % | 18.2 | 7.2 | 1.5 | 0.4 | 0.2 |
| Fe-150bar | Scale (tonne/day) | 0.1 | 1 | 10 | 100 | 500 |
| Total loop cost | million USD | 0.368 | 0.942 | 5.623 | 46.731 | 210.708 |
| Cost for separation | | 0.077 | 0.112 | 0.364 | 2.278 | 9.523 |
| Ratio for separation | % | 20.8 | 11.9 | 6.5 | 4.9 | 4.5 |
| Ru/C-100bar | Scale (tonne/day) | 0.1 | 1 | 10 | 100 | 500 |
| Total loop cost | million USD | 0.359 | 0.913 | 5.556 | 46.878 | 214.107 |
| Cost for separation | | 0.081 | 0.149 | 0.673 | 5.002 | 22.217 |
| Ratio for separation | % | 22.6 | 16.3 | 12.1 | 10.7 | 10.4 |
| Ru/C-75bar | Scale (tonne/day) | 0.1 | 1 | 10 | 100 | 500 |
| Total loop cost | million USD | 0.360 | 0.917 | 5.572 | 46.829 | 214.402 |
| Cost for separation | | 0.085 | 0.182 | 0.937 | 7.251 | 32.539 |
| Ratio for separation | % | 23.8 | 19.8 | 16.8 | 15.5 | 15.2 |
| Ru/C-50bar | Scale (tonne/day) | 0.1 | 1 | 10 | 100 | 500 |
| Total loop cost | million USD | 0.362 | 0.924 | 5.576 | 46.619 | 214.199 |
| Cost for separation | | 0.089 | 0.209 | 1.172 | 9.356 | 42.421 |
| Ratio for separation | % | 24.5 | 22.6 | 21.0 | 20.1 | 19.8 |

775

776